NMRF/VR/02/2023

VERIFICATION REPORT

NCUM Global Model Verification: Winter (DJF) 2022-23

K. Niranjan Kumar, Sukhwinder Kaur, M. Venkatarami Reddy, Harvir Singh, Sushant Kumar, Anumeha Dube, Mohana S. Thota, and Raghavendra Ashrit

2023

National Centre for Medium Range Weather Forecasting
Ministry of Earth Sciences, Government of India
A-50, Sector-62, NOIDA-201 309, INDIA

NCUM Global Model Verification:

Winter (DJF) 2022-23

K. Niranjan Kumar, Sukhwinder Kaur, M. Venkatarami Reddy, Harvir Singh, Sushant Kumar, Anumeha Dube, Mohana S. Thota, and Raghavendra Ashrit

NMRF/VR/02/2023

National Centre for Medium Range Weather Forecasting
Ministry of Earth Sciences, Government of India
A-50, Sector 62, NOIDA-201309, INDIA
www.ncmrwf.gov.in

Data Control Sheet

1	Name of the Institute	National Center for Medium range weather Forecasting
2	Document Number	NMRF/VR/02/2023
3	Date of Publication	November 2023
4	Title of the document	NCUM Global Model Verification: Winter (DJF) 2022-23
5	Type of the document	Verification Report
6	Number of pages, figures and Tables	53 pages, 38 figures, 4 Tables (including Appendix Figures and Tables)
7	Author (S)	K. Niranjan Kumar, Sukhwinder Kaur, M. Venkatarami Reddy, Harvir Singh, Sushant Kumar, Anumeha Dube, Mohana S. Thota, and Raghavendra Ashrit
8	Originating Unit	National Centre for Medium Range Weather Forecasting (NCMRWF), A-50, Sector-62, NOIDA201 309, India
9	Abstract	This report documents the performance of the global NCMRWF Unified Model (NCUM-G) analysis and forecast during the winter season (DJF) 2022-23. The verification results are presented to address both forecasters and model developers. The information on biases in the forecasted winds, temperature, humidity, rainfall, etc., is crucial for the forecasters to interpret the model guidance for accurate forecasting. Additionally, information on recent improvements in the model's skill contributes to bolstering confidence in the accuracy of the model forecasts.
10	References	17
11	Security classification	Unrestricted
12	Distribution	General

Table of Contents

NMRF/VR/02/2023

NCUM Global Model Verification: Winter (DJF) 2022-23

K. Niranjan Kumar, Sukhwinder Kaur, M. Venkatarami Reddy, Harvir Singh, Sushant Kumar, Anumeha Dube, Mohana S. Thota, and Raghavendra Ashrit

सारांश

यह रिपोर्ट सर्दियों के मौसम (दिसंबर से फरवरी) 2022-23 के दौरान वैश्विक रा.म.अ.मौ.पू.कें. यूनिफाइड मॉडल (एन.सी.यू.एम.-जी) विश्लेषण और पूर्वानुमान के प्रदर्शन का दस्तावेजीकरण करती है। सत्यापन परिणाम पूर्वानुमानकर्ताओं और मॉडल डेवलपर्स दोनों को संबोधित करने के लिए प्रस्तुत किए जाते हैं। सटीक पूर्वानुमान के लिए मॉडल मार्गदर्शन की व्याख्या करने के लिए पूर्वानुमानकर्ताओं के लिए पूर्वानुमानित हवाओं, तापमान, आर्द्रता, वर्षा आदि में पूर्वाग्रहों की जानकारी महत्वपूर्ण है। इसके अतिरिक्त, मॉडल के कौशल में हाल के सुधारों की जानकारी मॉडल पूर्वानुमानों की सटीकता में विश्वास बढ़ाने में योगदान देती है।

Abstract

This report documents the performance of the global NCMRWF Unified Model (NCUM-G) analysis and forecast during the winter season (DJF) 2022-23. The verification results are presented to address both forecasters and model developers. The information on biases in the forecasted winds, temperature, humidity, rainfall, etc., is crucial for the forecasters to interpret the model guidance for accurate forecasting. Additionally, information on recent improvements in the model's skill contributes to bolstering confidence in the accuracy of the model forecasts.

1. Introduction

This report documents the performance of the global NCMRWF Unified Model (NCUM-G) forecasts during the winter season (DJF) of 2022-23. The key objective of this assessment is to verify the forecasts' accuracy and reliability by comparing them to model analyses and observations. The results are summarized for the winter season to understand the average biases and forecast performances. The report is oriented towards both forecasters and model developers. Section 2 of the report elucidates the NCUM-G model description and the data assimilation system at NCMRWF, along with detailing the observed data utilized in this study. A comprehensive study of the seasonal mean analysis and corresponding anomalies is given in section 3, providing readers with a holistic view of the model's performance during the winter season. Section 4 delves into the systematic biases observed in the forecasted large-scale upper fields, specifically focusing on wind, temperature, humidity, rainfall, etc., which are expected to be useful for the forecasters to interpret the model forecasts, followed by a detailed validation of forecasts in section 5. Section 6 touches upon verification for significant weather events of DJF 2022-23. This includes verification for the Bay of Bengal (BoB) Severe Cyclonic Storm (SCS) 'Mandous' during 06-10 Dec 2022, which made landfall off the coast of Mamallapuram (a city in Tamil Nadu) on 9th Dec 2022. Section 7 provides a concise summary of the results.

2. NCMRWF Unified Modelling System & Verification datasets

2.1. Model Description

The NCMRWF started using the Unified Model (UM) Partnerships' seamless prediction system since 2012, designating it as NCUM. The operationalization of the NCMRWF global Numerical Weather Prediction (NWP) system (NCUM-G) commenced in 2012 with a grid resolution of 25 km (NCUM-G:V1) specifically tailored for medium-range weather prediction. This system underwent several upgrades, progressing to a 17 km horizontal resolution (NCUM-G:V3) in 2015, followed by further refinement to a 12 km resolution (NCUM-G:V5) in 2018. Subsequently, in 2020, the system transitioned to a 12 km resolution with enhanced model physics, designated as NCUM-G:V6. The present version (NCUM-G:V7) of NCUM-G has a horizontal grid resolution of ~12 km with 70 levels in the atmosphere reaching 80 km

height. It uses "ENDGame" dynamical core, which provides improved accuracy of the solution of primitive model equations and reduced damping. This helps in producing finer details in the simulations of synoptic features such as cyclones, fronts, troughs, and jet stream winds. ENDGame also increases variability in the tropics, which leads to an improved representation of tropical cyclones and other tropical phenomena. The model uses improved physics options of GA7.2 (Walters et al., 2017). An advanced data assimilation method of Hybrid 4-Dimensional Variational (4D-Var) is used for the creation of NCUM global analysis. The advantage of the Hybrid 4D-Var is that it uses a blended background error, a blend of "climatological" background error, and day-to-day varying flow dependent background error (derived from the 22–member ensemble forecasts). The hybrid approach is scientifically attractive because it elegantly combines the benefits of ensemble data assimilation (flow-dependent co-variances) with the known benefits of 4D-Var within a single data assimilation system (Barker, 2011). A brief description of the NCUM Hybrid 4D-Var system is given in Kumar et al. (2021, 2020, & 2019).

2.2. Observed/analysis Data used for the Verification

The seasonal mean analysis and anomalies are studied using the fifth-generation European Centre for Medium-Range Weather Forecasts (ECMWF) reanalysis product (ERA-5) data for the period 1979-2018 (Hershbach et al. 2020). The high resolution (12km) NCUM-G analysis data is interpolated to ERA-5 grid resolution (0.25^0 x 0.25^0). For verification of the forecasts, the NCUM-G model analysis is used. All systematic errors are computed at a native grid resolution of 12km.

Detailed quantitative rainfall forecast verification is based on the India Meteorological Department (IMD)-NCMRWF daily high resolution (0.25^0) rainfall analysis (Mitra et al. 2009, 2013). The rainfall analysis objectively analyses India Meteorological Department (IMD) daily rain gauge observations onto a 0.25^0 grid using a successive corrections technique with the GPM Satellite rainfall providing the first guess estimates. The model forecasts are gridded to the 0.25^0 observed rainfall grids over Indian land regions for 90 days from 1st December 2022 to 28th February 2023. As noted by Mitra et al. (2009), the merged analysis at 0.25^0 grid resolution is appropriate for capturing the large-scale rain features associated with the monsoon. The merging of the IMD gauge data into GPM estimates not only corrects the mean

biases in the satellite estimates but also improves the large-scale spatial patterns in the satellite field, which is affected by temporal sampling errors (Mitra et al. 2009). Verification of daily temperature forecasts is carried out against the IMD's daily observed gridded (0.5^0 x 0.5^0) maximum (Tmax) and minimum (Tmin) temperature data (Srivastava et al. 2009).

3. NCUM-G Analysis Mean and Anomalies during DJF 2022-23

3.1. Winds at 850, 700, 500, and 200 hPa levels

The NCUM-G mean analysis fields and anomalies relative to climatology are assessed in this section during DJF 2022-23. The discussion is presented for winds, temperature, and relative humidity at four standard pressure levels of 850, 700, 500, and 200 hPa. The anomalies are computed against the ERA5 climatology (1979-2018). The mean winds and anomalies at 850 and 700 hPa levels from NCUM-G analysis are shown in Figure 1a-d. At 850 hPa and 700 hPa, the NCUM-G model seasonal mean analysis represents northeasterly to easterly winds with increasing altitudes having strength ranging from 4 to 8 m/s. The westerly wind strength increases with altitude having magnitudes which is about 8 -10 m/s at 700 hPa (Figures 1a and 1b). This wind flow brings in moisture from the Arabian Sea (AS) during winter which provides suitable moisture incursion for increased precipitation in association with Western Disturbances (WDs). In contrast to the westerlies in the north, easterlies prevail in south India subsequently creating an anticyclonic circulation clearly visible over the central India in the NCUM-G model analysis. The anomalous conditions for the DJF 2022-23 winter period are estimated by removing the climatological ERA5 reanalysis from the NCUM-G seasonal mean winds. The mean anomalous winds at 850 hPa and 700 hPa are shown in Figures 1c-d. The anomalies indicate contrasting features in north and south with weaker and stronger winds in NCUM-G analysis with respect to ERA5 reanalysis, respectively, over the Indian subcontinent. On the other hand, over the equatorial Indian Ocean, specifically in southern latitudes, the winds are extremely higher with magnitudes of about 5-10m/s in NCUM-G analysis. Overall, in north India where the rainfall is higher in the winter period, the magnitude of winds is relatively lower compared to ERA5 reanalysis due to persistent anomalous easterlies (Figure 1).

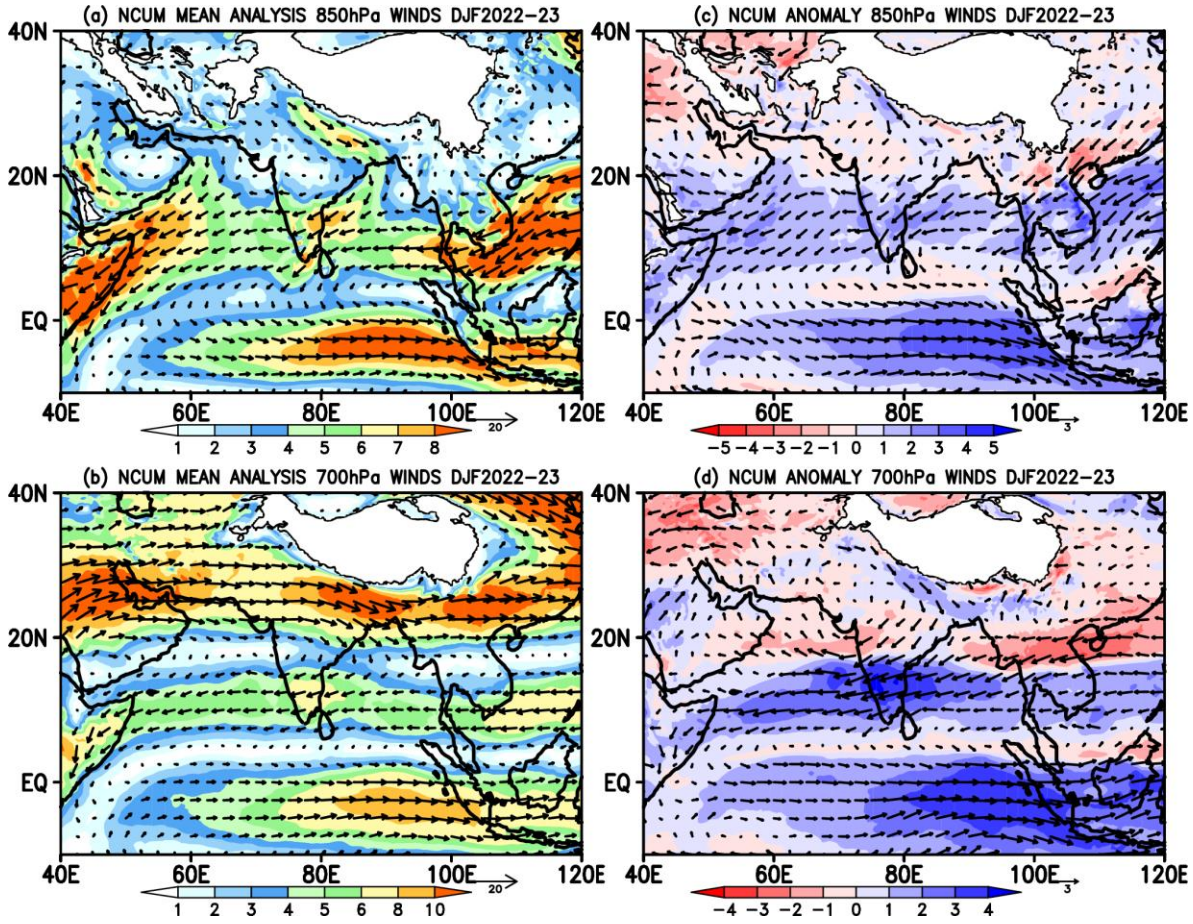

Figure 1. Mean winds at (a) 850 hPa and (b) 700 hPa in the NCUM-G Analysis during DJF 2022-23 (m/s). Right panels show the anomaly circulations at (c) 850 hPa and (d) 700 hPa.

The mean winds from NCUM-G model analysis at 500 hPa and 200 hPa, representative of mid- and upper troposphere is shown in Figures 2a and 2b, respectively. As increasing the altitudes, the mean winds in the north Indian region getting more strengthened from ~16m/s at 500hPa to more than 40m/s in the upper troposphere. Hence, the NCUM-G model analysis could represent the upper-level subtropical westerly jet (STWJ) at 200 hPa. This is one of the important winter seasonal wind features which brings in enormous amount of precipitation in association with WDs as it provides necessary divergence for the intensification of the WDs. At the same time, weak easterlies prevail in the south Indian region (Figures 2a and 2b). The associated anomalous winds in the model analysis are shown in Figures 2c and 2d with respect to ERA5 reanalysis. In the mid- and upper troposphere, the winds are relatively lower

compared to climatology in the north Indian while stronger in the south Indian region. The anomalous easterlies are clearly discernible prevailing from the west Pacific to Middle Eastern region in the upper troposphere over the north India. Presence of these anomalous easterlies extending from west Pacific to Middle Eastern regions indicate that the subtropical westerlies are slightly weaker at 200 hPa level in NCUM-G during DJF 2022-23 winter (Figure 2d). In the equatorial regions, the upper tropospheric winds are quite strong with magnitudes of more than 6m/s in winter 2022-23.

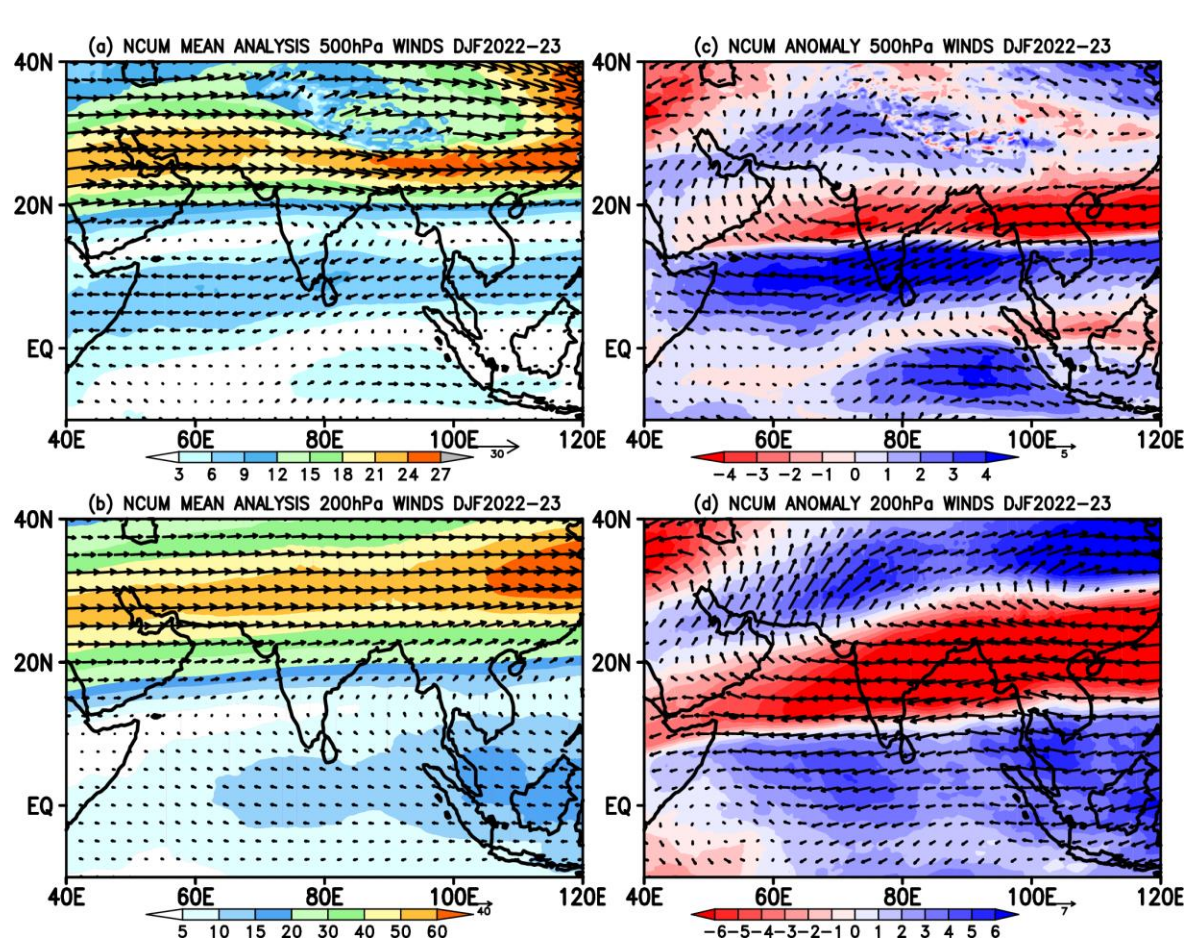

Figure 2. Mean winds at (a) 500 hPa and (b) 200 hPa in the NCUM-G Analysis during DJF 2022-23 (m/s). Right panels show the anomaly circulations at (c) 500 hPa and (d) 200 hPa.

3.2. Temperature at 850, 700, 500, and 200 hPa levels

The spatial distribution of seasonal mean temperature is shown in Figure 3. Usually, the cold weather season sets in by mid-November in northern India. December and January are the coldest months in the northern plain. The mean daily temperature remains below 21^0C over most parts of northern India (Figure 3a). The Peninsular region of India, however, does not have any well-defined cold weather season but the temperature usually rises as we move from north to south (Figure 3a). Similar daily mean temperature patterns are also seen at 700 hPa (Figure 3b). The anomalous temperatures in the lower troposphere (850 hPa and 700 hPa, Figures 3c and 3d) indicate the winter of 2022-23 is warmer than the climatology with magnitudes between 1-2 ^{0}C in north India. The warmer temperatures stretch from northwest to southeast India covering the Indo-Gangetic plains. The anomalous warm temperatures over northern and central parts of Indian is due to the large-scale adiabatic descent induced by anti-cyclonic circulation extending from 850 to 200 hPa levels. With increasing pressure levels, the mean temperature distribution at 500 hPa and 200 hPa drastically decreases (Figures 4a and 4b). At 200 hPa, the temperatures are nearly uniform throughout the country. Nevertheless, the temperature anomalies in north India still indicate warmer than the climatology (Figures 4c and 4d).

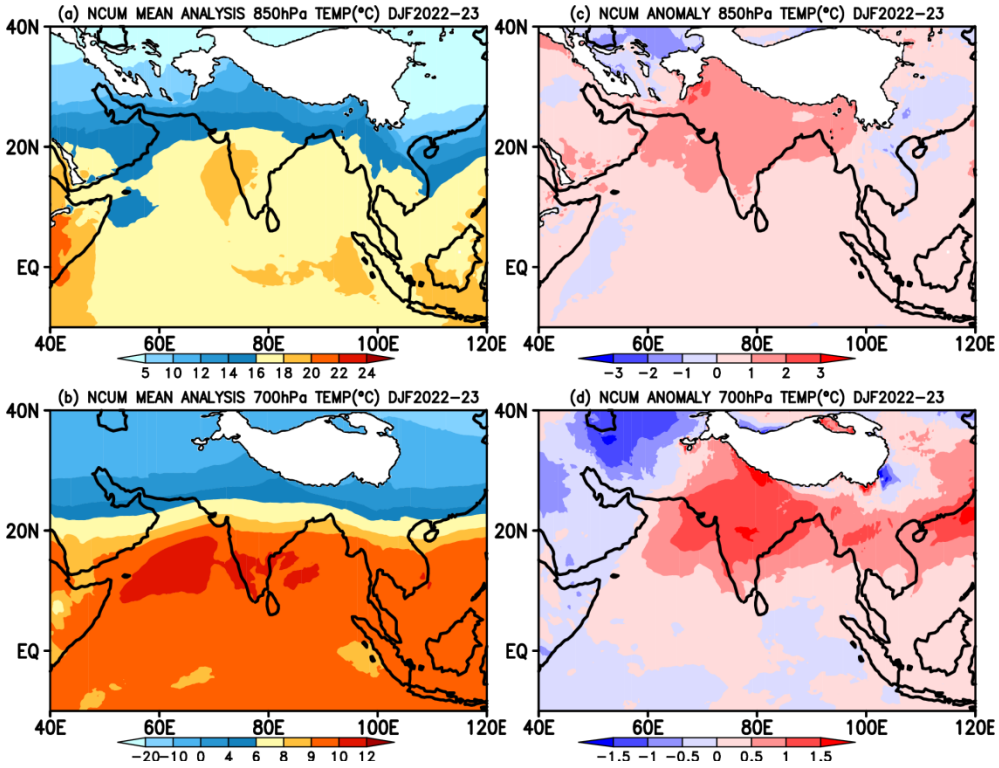

Figure 3. Mean Temperature (Degree Celsius, ^{0}C) at (a) 850 hPa and (b) 700 hPa in the NCUM-G Analysis during DJF 2022-23. Right panels show the Temperature anomalies at (c) 850 hPa and (d) 700 hPa.

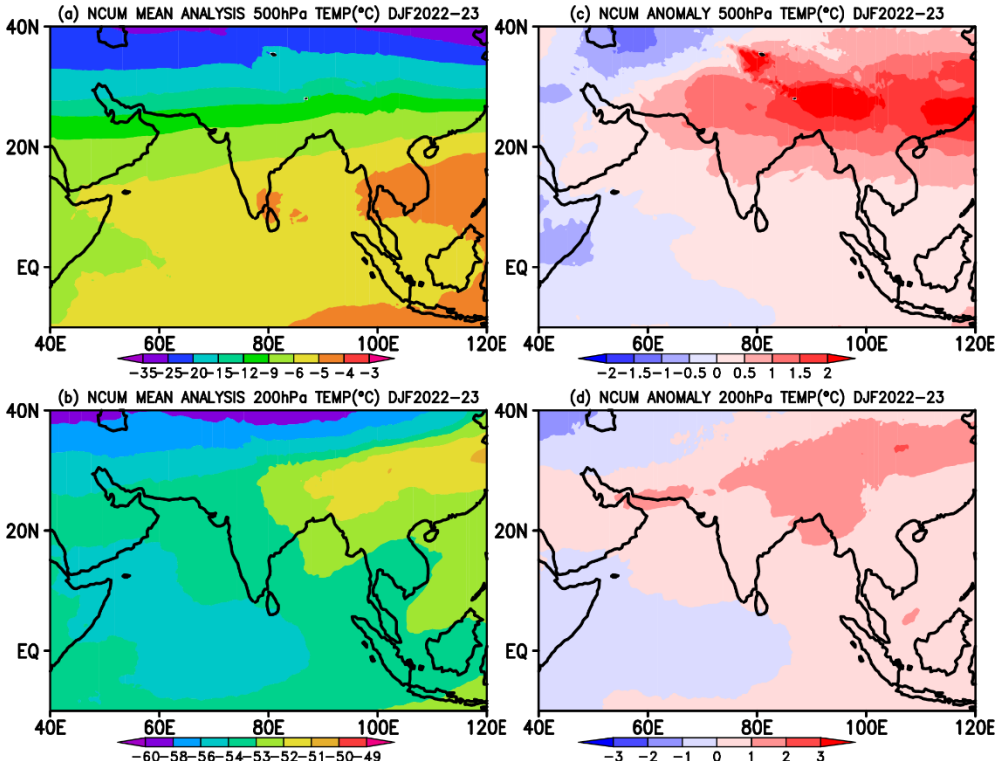

Figure 4. Mean Temperature (Degree Celsius, ^{0}C) at (a) 500 hPa and (b) 200 hPa in the NCUM-G Analysis during DJF 2022-23. Right panels show the Temperature anomalies at (c) 500 hPa and (d) 200 hPa.

3.3. Relative Humidity (RH) at 850, 700, and 500 hPa levels

The distribution of humidity is an important field along with winds and temperature for controlling the rainfall. Hence, we further show the spatial distribution of seasonal mean RH from NCUM-G model analysis in Figures 5a (850 hPa) and 5b (700 hPa). Most of the northern part of India is quite dry due to cold dry air blowing from the north during the winter, while the RH is relatively higher in the south Indian region at 850 hPa (Figure 5a). Meanwhile, at 700 hPa, mean RH exhibits dry conditions over the Indian land region (Figure 5b). When we investigate the anomalies, the DJF 2022-23 indicates a lower percentage of RH compared to the climatology over the entire Indian land region (Figures 5c and 5d). The Oceanic regions of the Bay of Bengal (BoB) and Arabian Seas also showed positive anomalies in the humidity distribution for the winter period. At the same time, negative anomalies are noted in the equatorial regions.

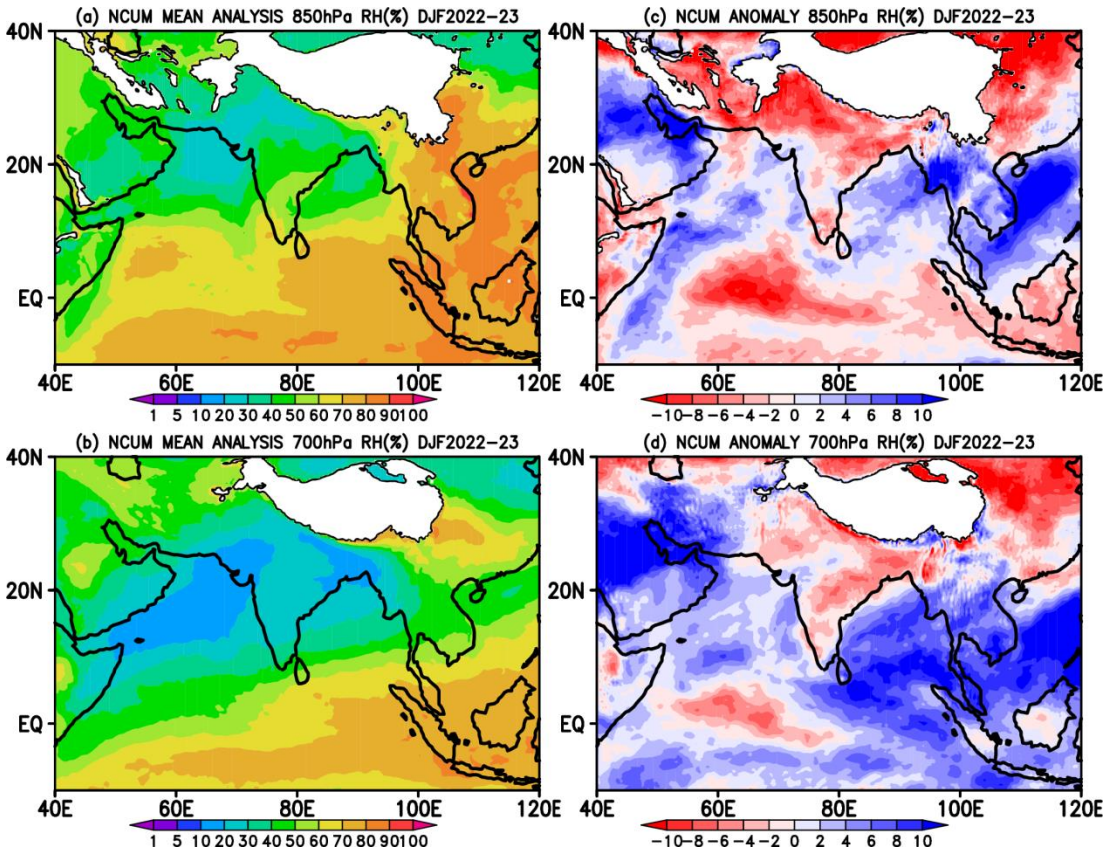

Figure 5. Mean Relative Humidity (%) at (a) 850 hPa and (b) 700 hPa in the NCUM-G Analysis during DJF 2022-23. The right panels show the anomalies in Relative Humidity at (c) 850 hPa and (d) 700 hPa.

Further, we also showed in Figure 6, the spatial distribution of RH in the mid troposphere at 500 hPa level. The seasonal mean distribution of RH indicates dry conditions over the Indian Subcontinent. Nevertheless, occasionally the RH can be increased due to movement of synoptic-scale disturbances in the north Indian winter during which the RH will be increased significantly. These incremental RH values (excess moisture in the column) induce thermodynamic instability over these regions favouring convection initiation. On the other hand, in the oceanic regions, specifically in the maritime continent, a significant amount of the available moisture with RH magnitudes of more than 60% can be noticed. The anomalous RH distribution is shown in Figure 6 (right panel). The south Indian region shows some positive anomalies in RH with respect to climatology, but it may not be significant as the mean RH

itself is extremely low. However, negative RH anomalies can be noticed over the maritime continent where the mean distribution is generally higher.

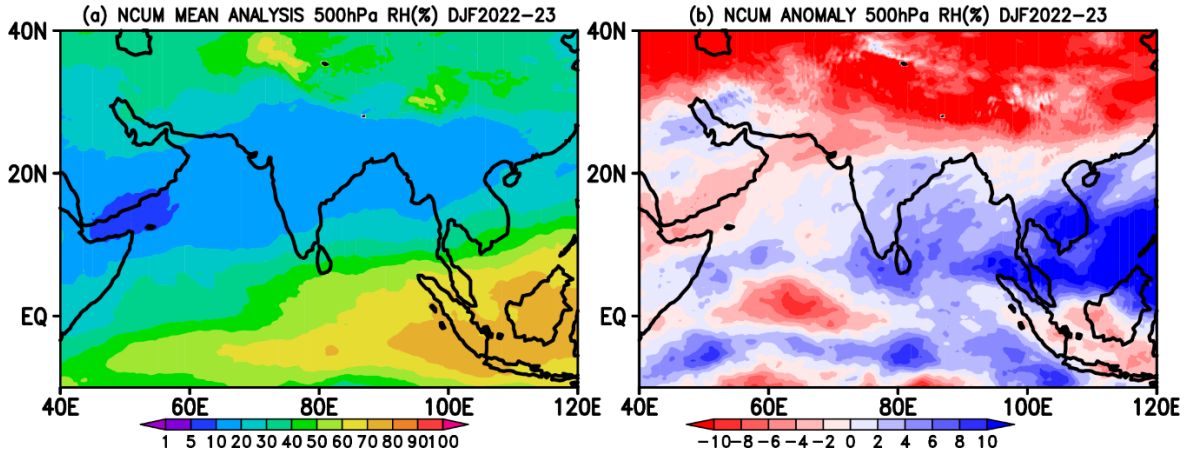

Figure 6: Mean Relative Humidity (%) at (a) 500 hPa in the NCUM-G Analysis during DJF 2022-23. The right panel shows the anomalies in Relative Humidity at (b) 500 hPa.

4. Systematic Errors in NCUM-G Forecasts

In this section, the systematic errors in Day-1 (24 hr), Day-3 (72 hr), and Day-5 (120 hr) forecasts during DJF 2022-23 are briefly described. In addition, the forecast errors with respect to model analysis are also presented for Winds and Temperature at 850, 700, 500, and 200 hPa levels; and Relative Humidity at 850 and 700 hPa levels (Figures 7-16).

4.1. Winds at 850, 700, 500, and 200 hPa levels

Mean winds at 850 hPa level show the presence of low-level anticyclonic circulation over the central Indian region with westerlies and easterlies on the north and southern planks, respectively. Northeasterly winds are prominently seen over the Bay of Bengal and AS regions. Maximum northeasterly winds are observed along the coastal regions of Somalia and the South China Sea. In addition, the presence of strong westerly winds south of the equator is also noted. Systematic errors in winds from Day-1 forecasts at this level show an easterly wind bias over the south Bay of Bengal. A westerly wind bias over the south of the equator around 60^0E and easterly wind bias around the maritime continent (MC) is also noted (Figures 7b-d). With forecasts lead time these errors in low-level winds increases and this could be due to the enhanced convective activity around the equatorial regions during winter season (Figures 7b-d). Similar systematic errors in winds are also noticed at 700 hPa level. Interestingly Day-1

forecast errors are relatively small compared to the Day-3 and Day-5 forecasts (Figures 8b-d). In addition, westerly wind bias is more prominent at 700 hPa level over central India and the northeastern regions in Day-3 and Day-5 forecasts (Figures 8c-d).

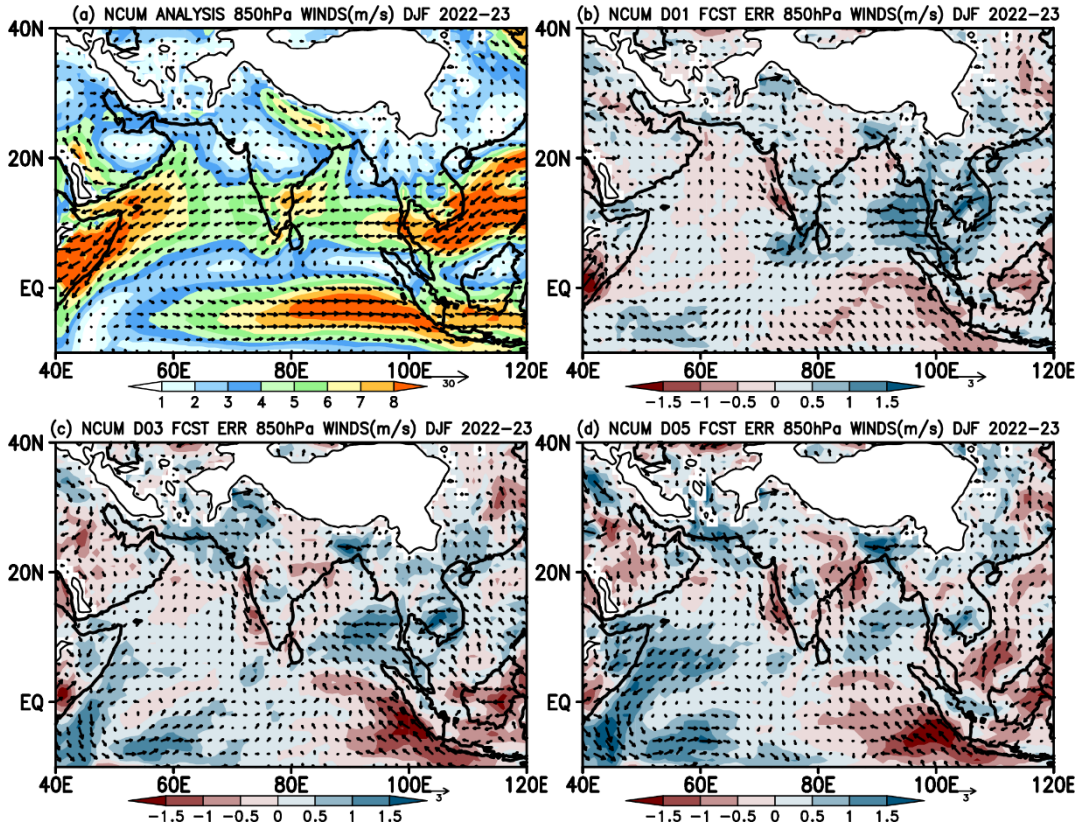

Figure 7. (a) Mean winds and systematic errors (m/s) in (b) Day-1, (c) Day-3, and (d) Day-5 forecasts at 850 hPa during DJF 2022-23.

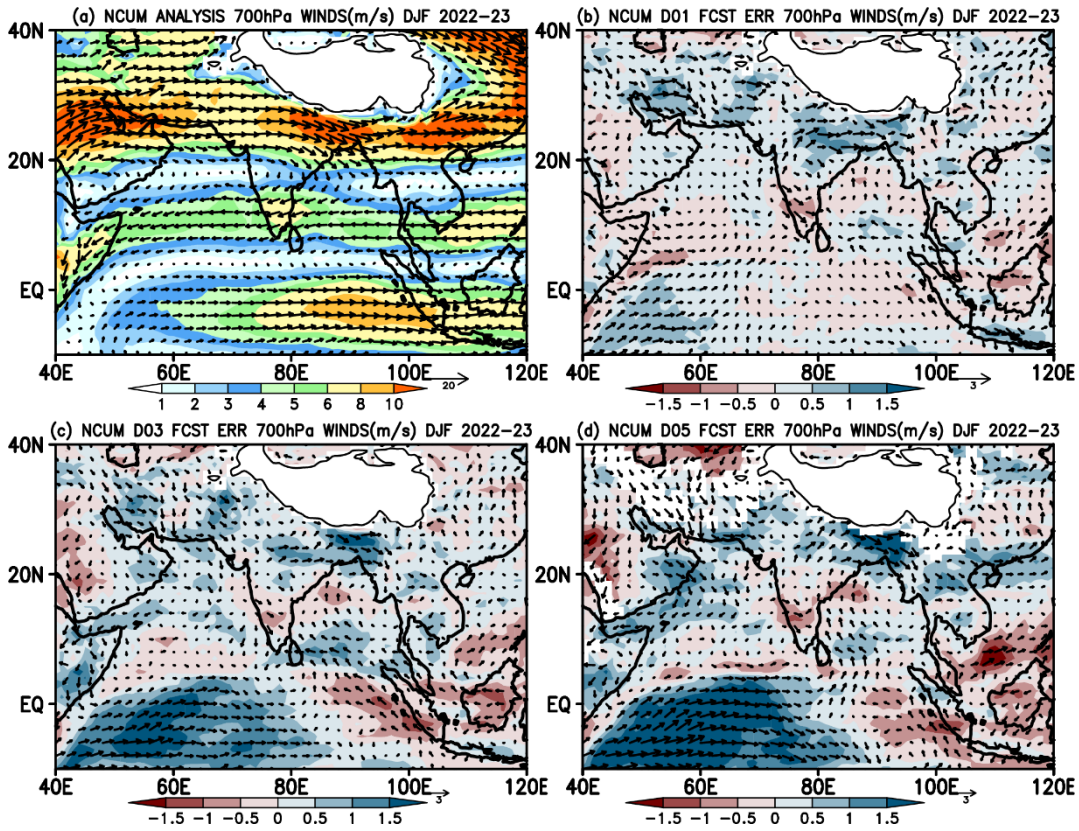

Figure 8. (a) Mean winds and systematic errors (m/s) in (b) Day-1, (c) Day-3, and (d) Day-5 forecasts at 700 hPa during DJF 2022-23

Mean winds at 500 hPa level (Figure 9a) show strong westerlies between 30-40^{0}N and these westerly winds penetrated over the central Indian region. Errors in winds at 500 hPa level are relatively small in Day-1 forecasts. The westerly wind bias over northern parts of India and easterly wind bias in the south Bay of Bengal and AS seems enhancing in Day-3 and Day-5 forecasts. The enhanced winds exhibit cyclonic circulation just above equator in Day-5 forecast around 500hPa level, which is noteworthy (Figures 9b-d). Systematic errors at 200 hPa level winds show enhanced divergent circulation centered around central parts of India in Day-3 forecasts and similar spatial pattern in winds is also seen in Day-5 forecasts with enhanced error magnitudes (Figures 10 c-d). These enhanced divergent circulations over central parts of India is due to the reduction in the strength of subtropical westerlies with forecasts lead time.

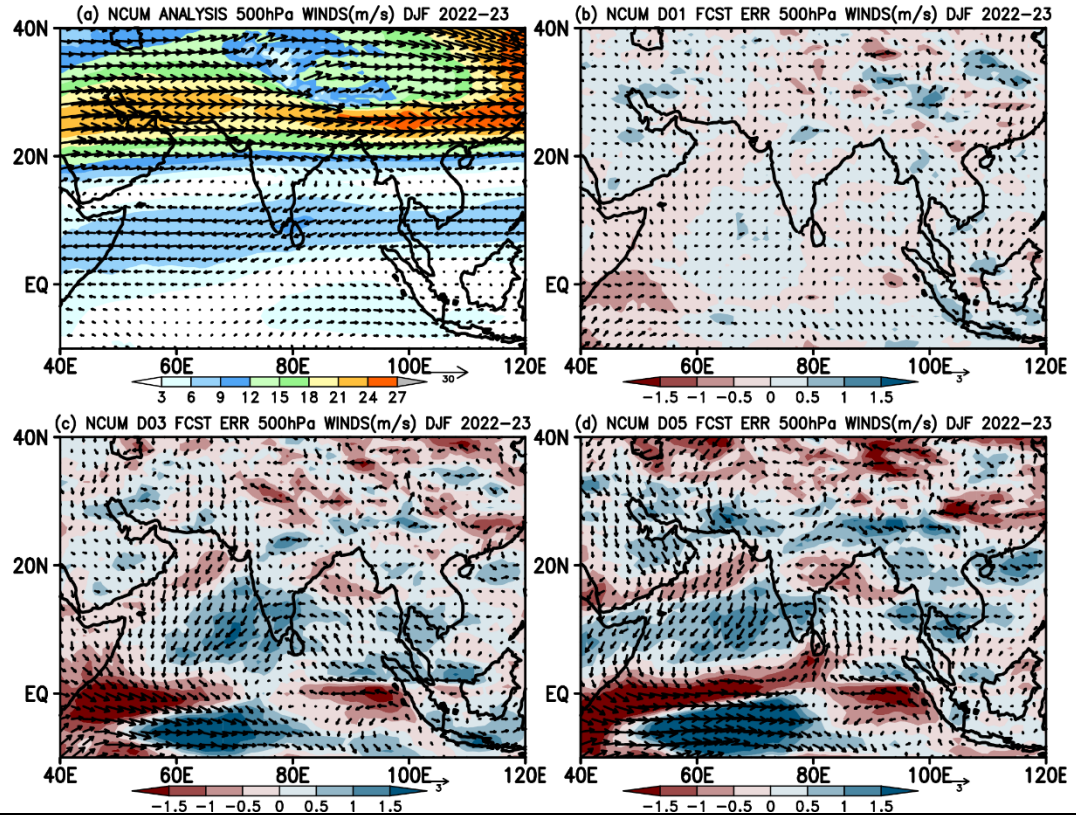

Figure 9. (a) Mean winds and systematic errors (m/s) in (b) Day-1, (c) Day-3, and (d) Day-5 forecasts at 500 hPa during DJF 2022-23.

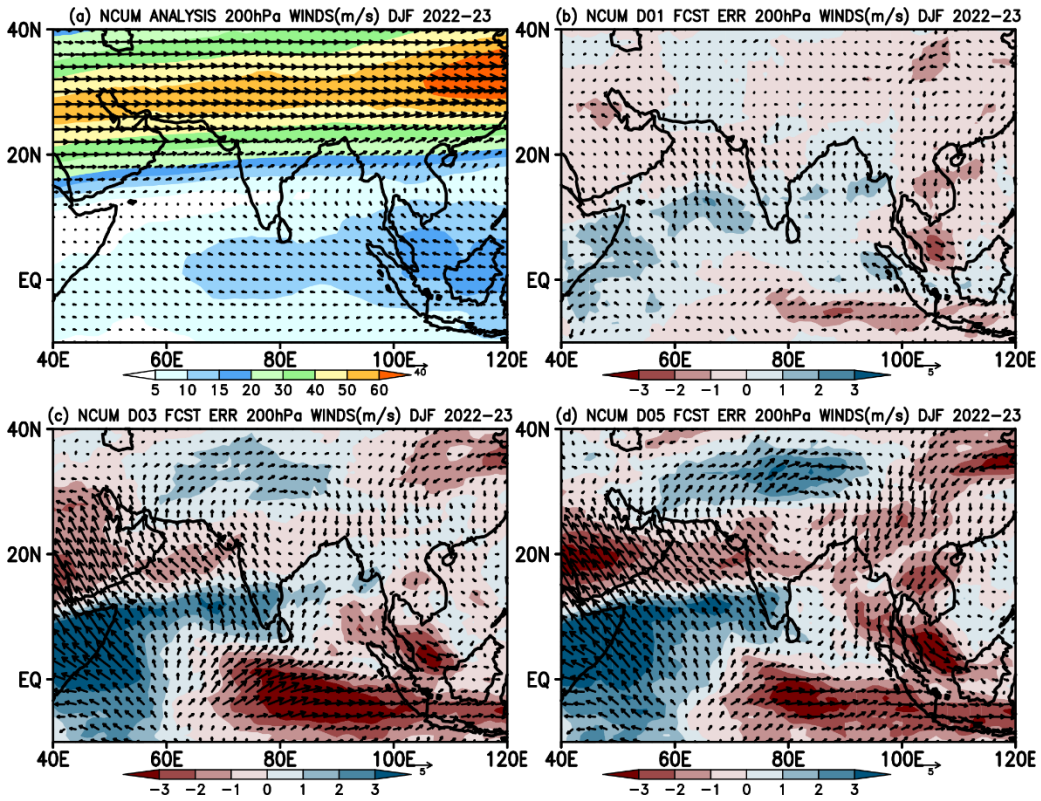

Figure 10. (a) Mean winds and systematic errors (m/s) in (b) Day-1, (c) Day-3, and (d) Day-5 forecasts at 200 hPa during DJF 2022-23.

4.2. Temperature and Relative Humidity

Spatial map of seasonal mean temperature from NCUM-G analysis at 850 hPa shows warm and cold temperatures, respectively, over the southern and northern land regions of India including surrounding oceanic regions (Figure 11a). Model shows warm bias (~1 ^{0}C) over most of the Indian land mass and the magnitude of this bias increases with forecasts lead time (Figures 11 c-d). The error increments at 850 hPa temperatures are also more prominent over the eastern African regions. On a similar note, the temperature at 700 hPa shows warm bias (~0.5 ^{0}C) over the northern and central Indian regions. The warm bias seen at both 850 and 700 hPa levels over the central Indian region is due to the presence of anti-cyclonic circulation throughout the column and associated adiabatic warming. Interesting to see that the bias over the BoB region reverse sign and now exhibits cold bias compared to the 850 hPa level. This cold bias over BoB is consistent in all the forecast lead times up to Day-5 (Figures 12 c-d).

Systematic errors at 500 and 200 hPa levels show warm and cold bias, respectively, over the Indian land region including surrounding oceanic regions (Figures 13 c-d and Figures 14 c-d). The cold bias over central Indian region at 200 hPa level is perhaps due to the presence of anticyclonic circulation which brings cold air from midlatitudes at northward flank (Figures 10 c-d).

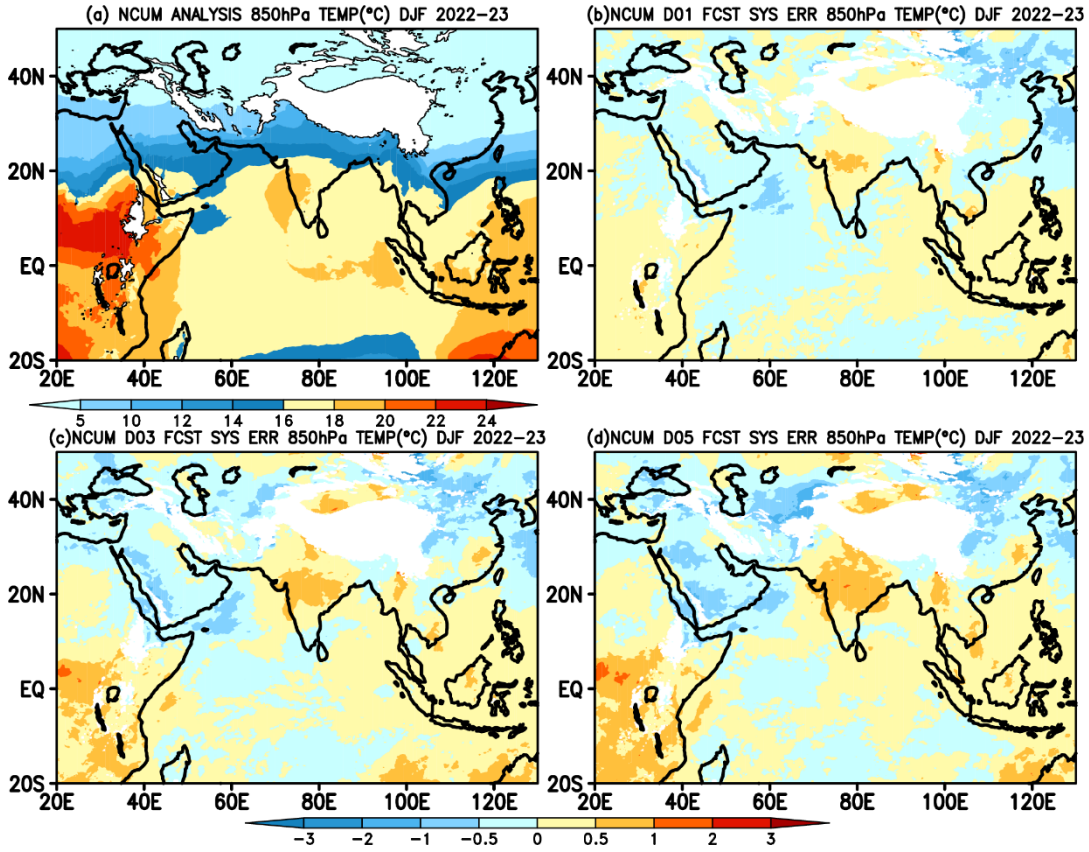

Figure 11. (a) Mean Temperature and systematic errors (Degree Celsius, ^{0}C) in (b) Day-1, (c) Day-3, and (d) Day-5 forecasts at 850 hPa during DJF 2022-23.

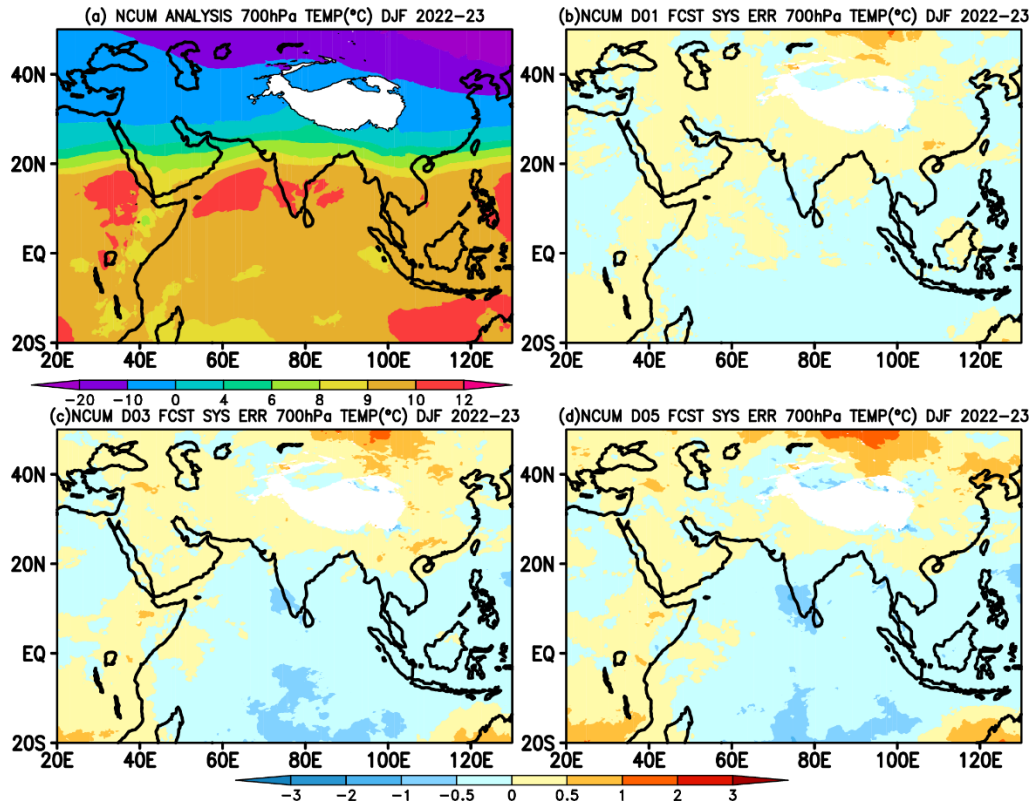

Figure 12. (a) Mean Temperature and systematic errors (Degree Celsius, ^{0}C) in (b) Day-1, (c) Day-3, and (d) Day-5 forecasts at 700 hPa during DJF 2022-23.

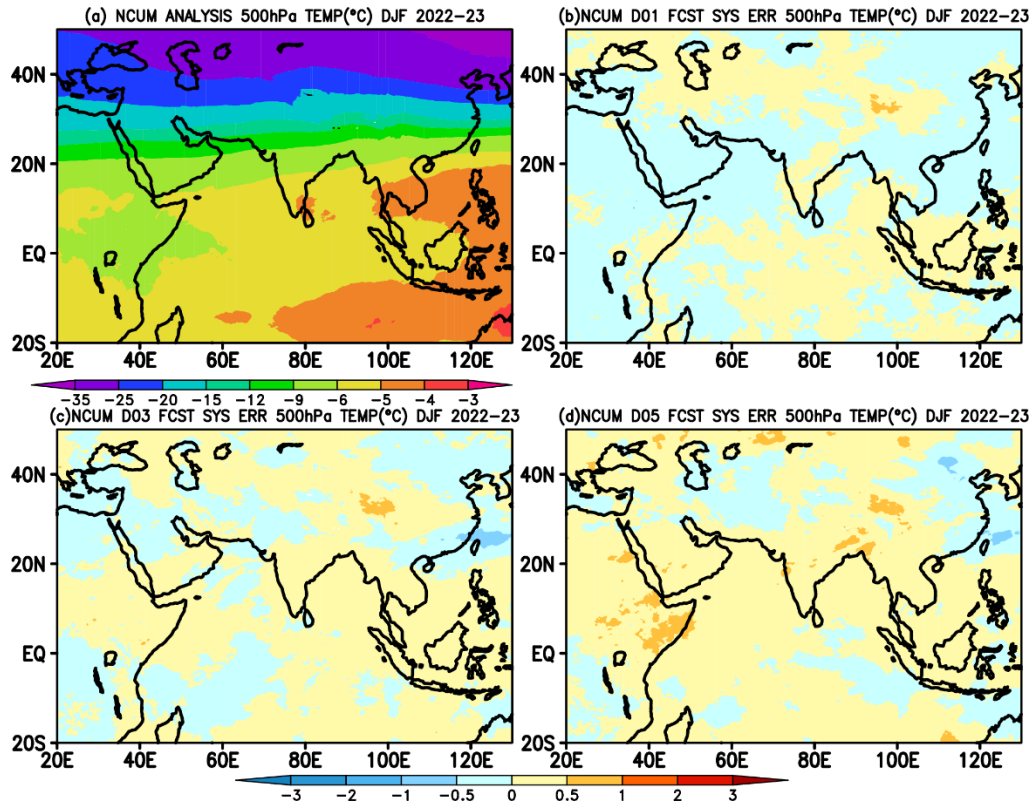

Figure 13. (a) Mean Temperature at and systematic errors (Degree Celsius, ^{0}C) in (b) Day-1, (c) Day-3, and (d) Day-5 forecasts at 500 hPa during DJF 2022-23.

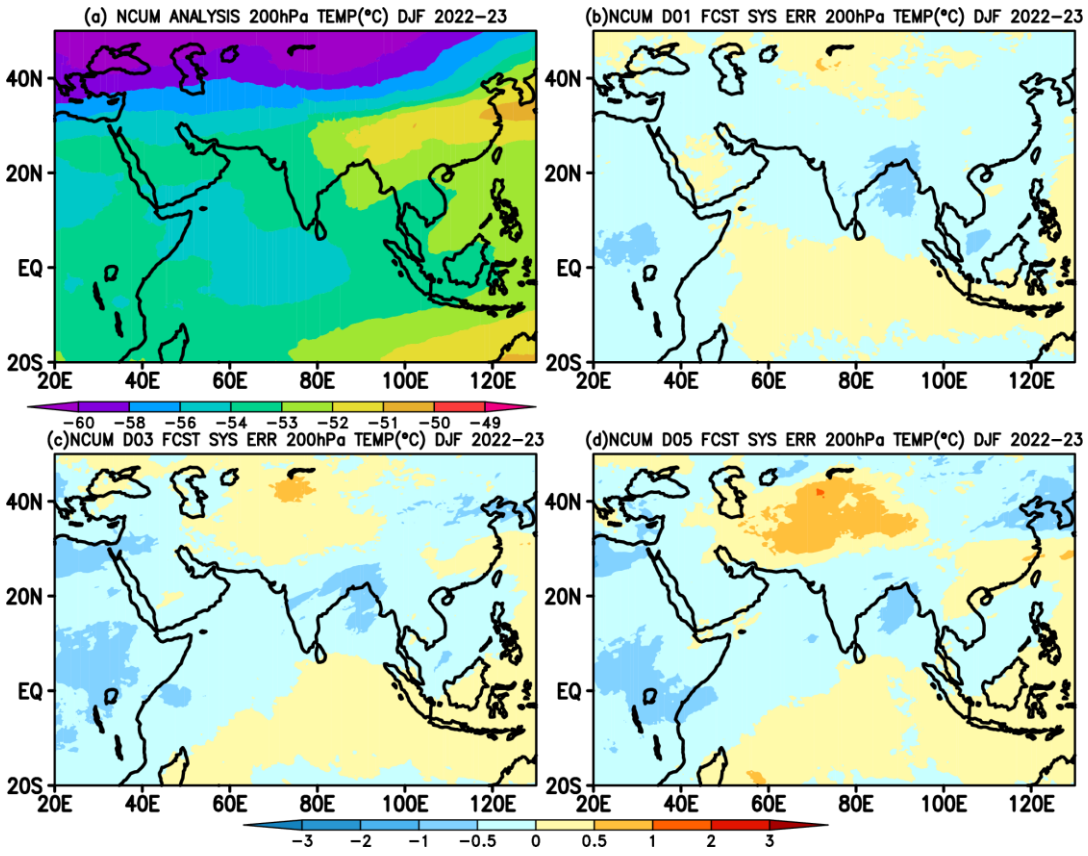

Figure 14. (a) Mean Temperature and systematic errors (Degree Celsius, ^{0}C) in (b) Day-1, (c) Day-3, and (d) Day-5 forecasts at 200 hPa during DJF 2022-23.

Seasonal mean RH at 850 hPa (Figure 15) and 700 hPa (Figure 16) levels show large values > 90% over equatorial regions and relatively less RH values over northern parts of the Indian subcontinent. Maximum in RH values are concentrated over MC. Systematic errors show large dry bias over the Indian land regions at 850hPa level and this dryness is enhancing with forecasts lead time (Figures 15c-d). Omni presence of strong north easterlies over open oceanic regions of AS and BoB, and increased evaporation could be one primary reason for the positive RH values over these regions (Figures 15c-d). In contrary, most of the Indian subcontinent and surrounding oceanic regions exhibit moist bias as evidenced by positive RH values, except Africa, the South China Sea, MC, and south of the equator regions. Interestingly the dry bias observed over the Indian land region at 850 hPa level change sign to positive and moist bias is seen at 700 hPa level. Additionally, the moist bias south of the equator is getting intensified

in the Day-3 and Day-5 forecast and the entire column is occupied with excess moisture at 700 hPa levels (Figures 16 b-d).

In the next section, a brief description of systematic errors in the model forecasts is presented for key surface variables such as 2m Temperature (Figure 17), 10m winds (Figure 18), and Total Precipitable Water (PWAT; Figure 19). The errors are computed against the NCUM-G analysis.

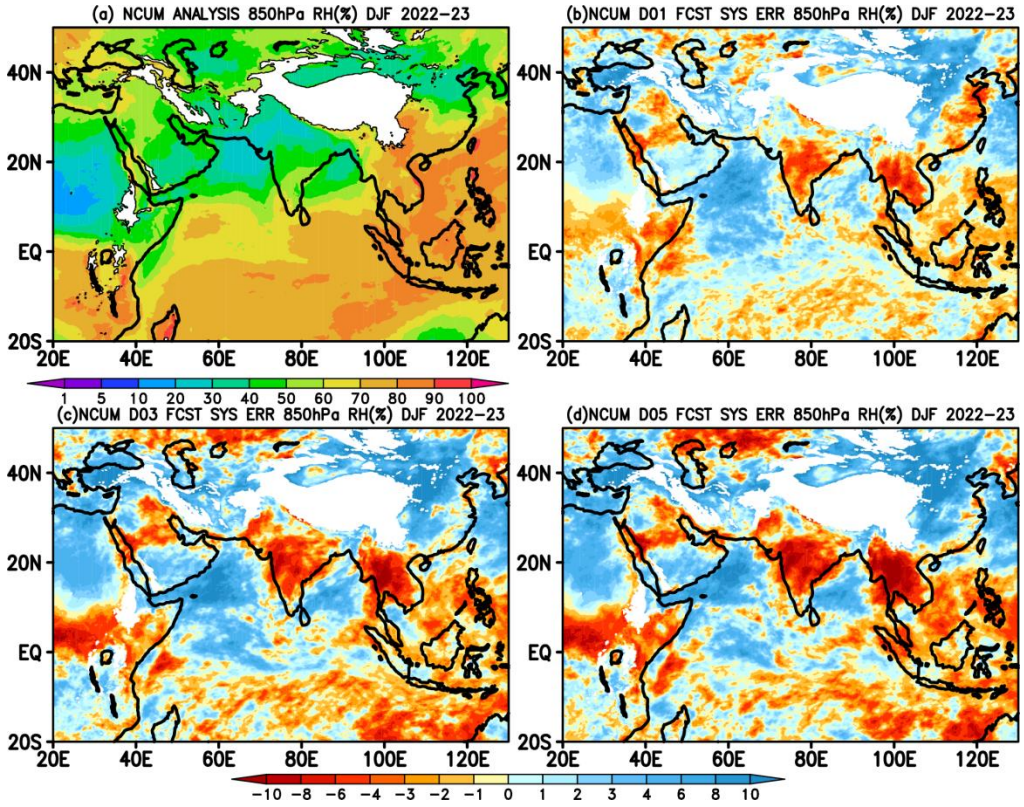

Figure 15. (a) Mean Relative Humidity and systematic errors (%) in (b) Day-1, (c) Day-3, and (d) Day-5 forecasts at 850 hPa during DJF 2022-23.

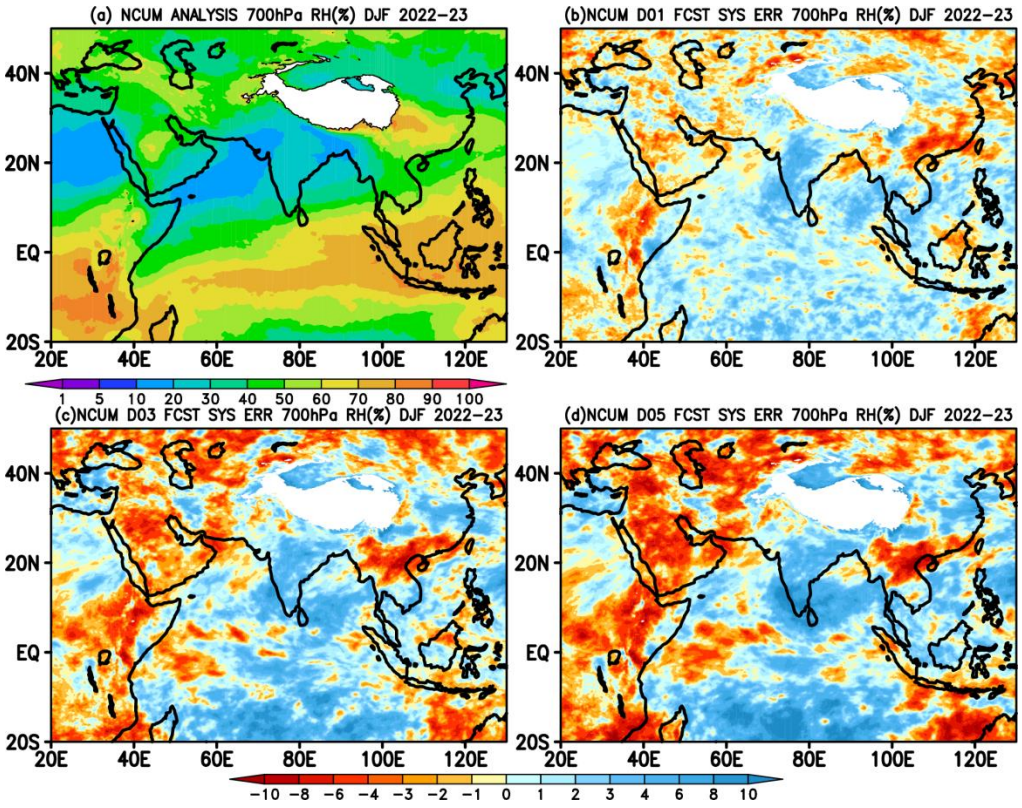

Figure 16. (a) Mean Relative Humidity and systematic errors (%) in (b) Day-1, (c) Day-3, and (d) Day-5 forecasts at 700 hPa during DJF 2022-23.

4.3. Surface (10m) winds

Seasonal mean winds at 10m from the analysis show the presence of strong North easterlies over the Bay of Bengal (BoB) and Arabian Sea (AS) with maximum winds around open AS, the African coast, and the South China Sea. Reversal of these north easterlies to westerlies after crossing the equator is also noted in the analysis (Figure 17a). The systematic errors in the forecasts (Figures 17 b-d) depict few notable features; 1) The North easterlies which are noticed on Day-1 (Figure 17b) changed their direction to southerlies with lead time and it is clearly seen on Day-5 (Figure 17d). 2) The north-westerly wind bias over northern AS in Day-1 is enhancing its strength with forecasts lead time. 3) On a similar note, the easterly wind bias seen over south of the equator around ~100 ^{0}E is also getting intensified with forecast lead time (Figures 17b-d).

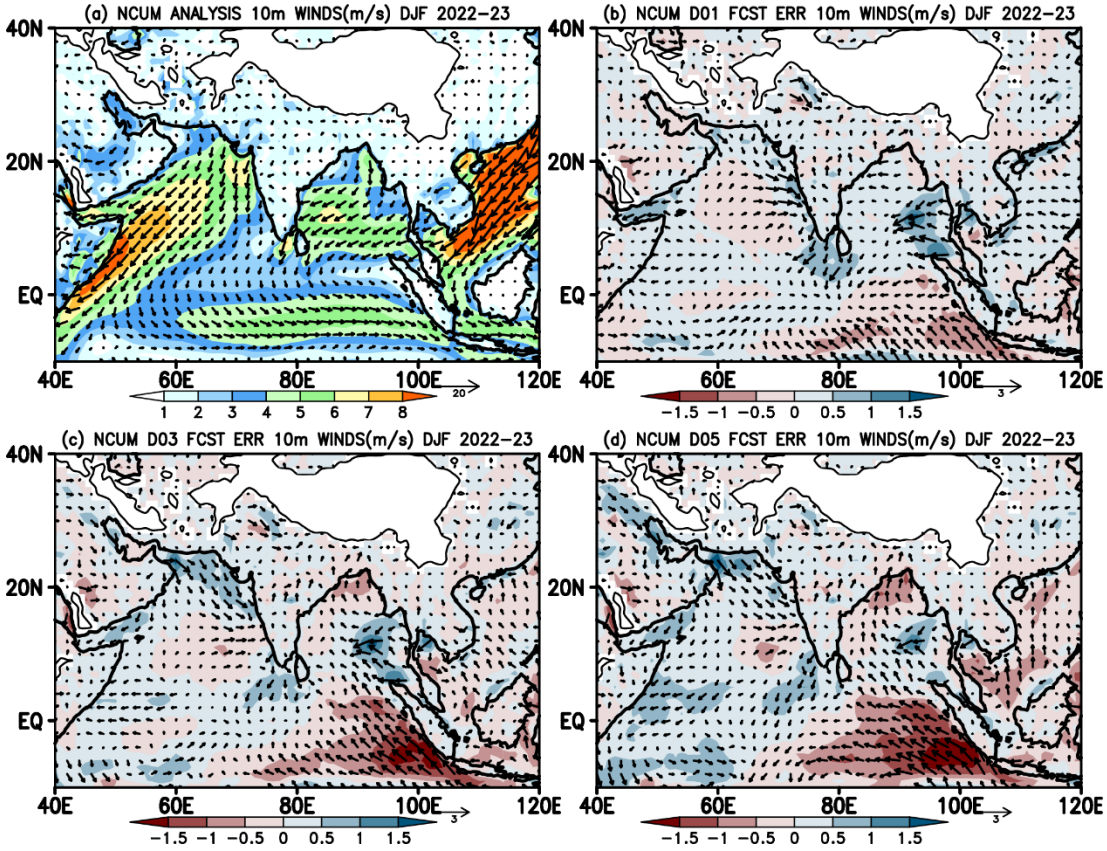

Figure 17. (a) Mean winds at 10m height and systematic errors (m/s) in (b) Day-1, (c) Day-3, and (d) Day-5 forecasts during DJF 2022-23.

4.4. Temperature at 2m

Seasonal temperature patterns over the Indian region show cold temperatures (12-15 ^{0}C) in the north and warm temperatures (>25 ^{0}C) towards the south (Figure 18a). Systematic errors (Figures 18 b-d) show a relatively warm bias over Indian land regions and north of 40 ^{0}N latitude regions. Interestingly these warm biases are increasing with forecast lead time, especially over Indian region. This can be attributed to the dry north -westerly winds from Northwest entering into Indian land and north AS (Figures 18 c-d). In addition, most of the oceanic regions of the BoB and AS exhibited warm bias of the range 0-0.5 ^{0}C in all the forecast lead times. It is noted that the magnitude of the bias is increasing with forecasts lead time, which is noteworthy.

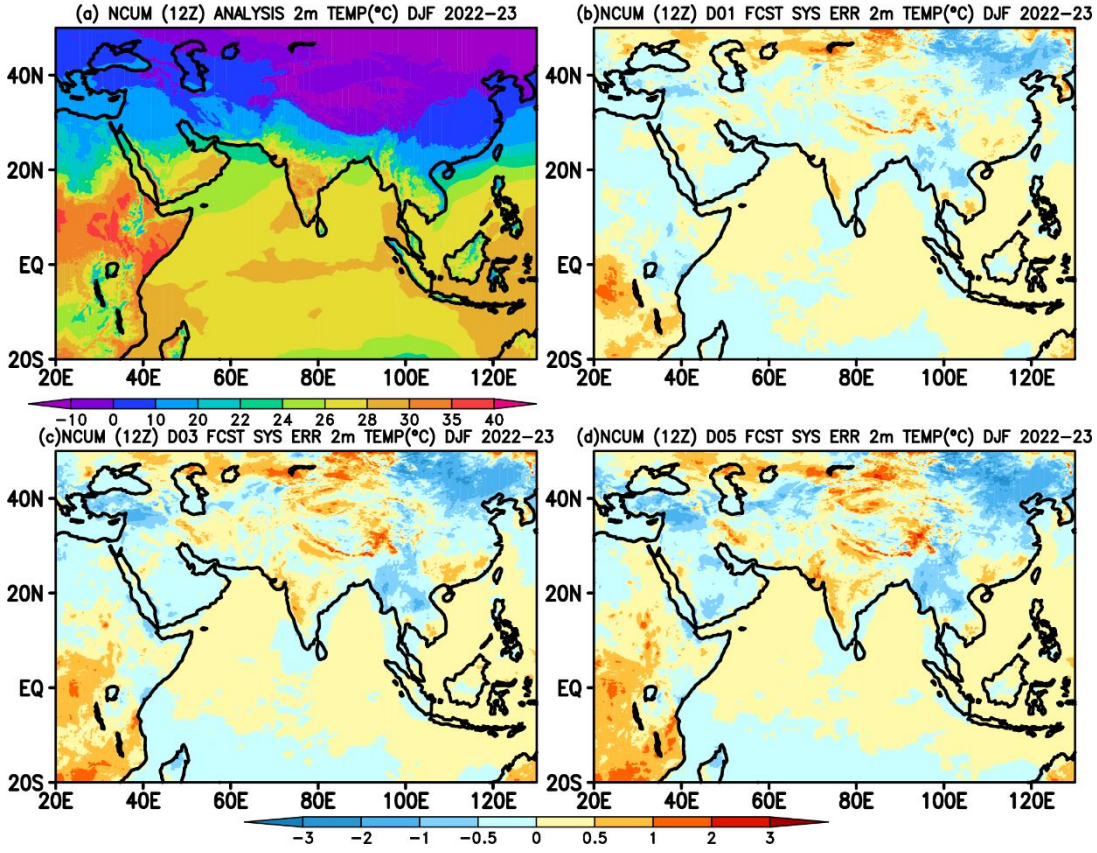

Figure 18. (a) Mean Temperature at 2m height and systematic errors (Degree Celsius, ^{0}C) in (b) Day-1, (c) Day-3, and (d) Day-5 forecasts during DJF 2022-23.

4.5. Total Precipitable Water (PWAT)

Seasonal mean PWAT shows a large value (> 60 mm) around the equatorial regions (Figure 19a), especially over the Maritime continent owing to the presence of winter-time MJO active conditions over these regions. In contrast, most of the northern and central Indian regions are dry with very less PWAT values (5-15 mm). However, extreme southeast peninsular India exhibits moderate PWAT values around 35-40 mm due to the effect of northeast monsoon conditions (Figure 19a). Systematic error in PWAT (Figures 19 b-d) shows a column dry over the northern and central Indian regions on Day-1, this dryness in column is enhanced with forecast lead time, and its magnitude is maximum on Day-5 (Figures 19 c-d). Large positive PWAT biases are seen over BoB, AS, and over equatorial regions. This excess column water could be one reason for excess rainfall over these regions.

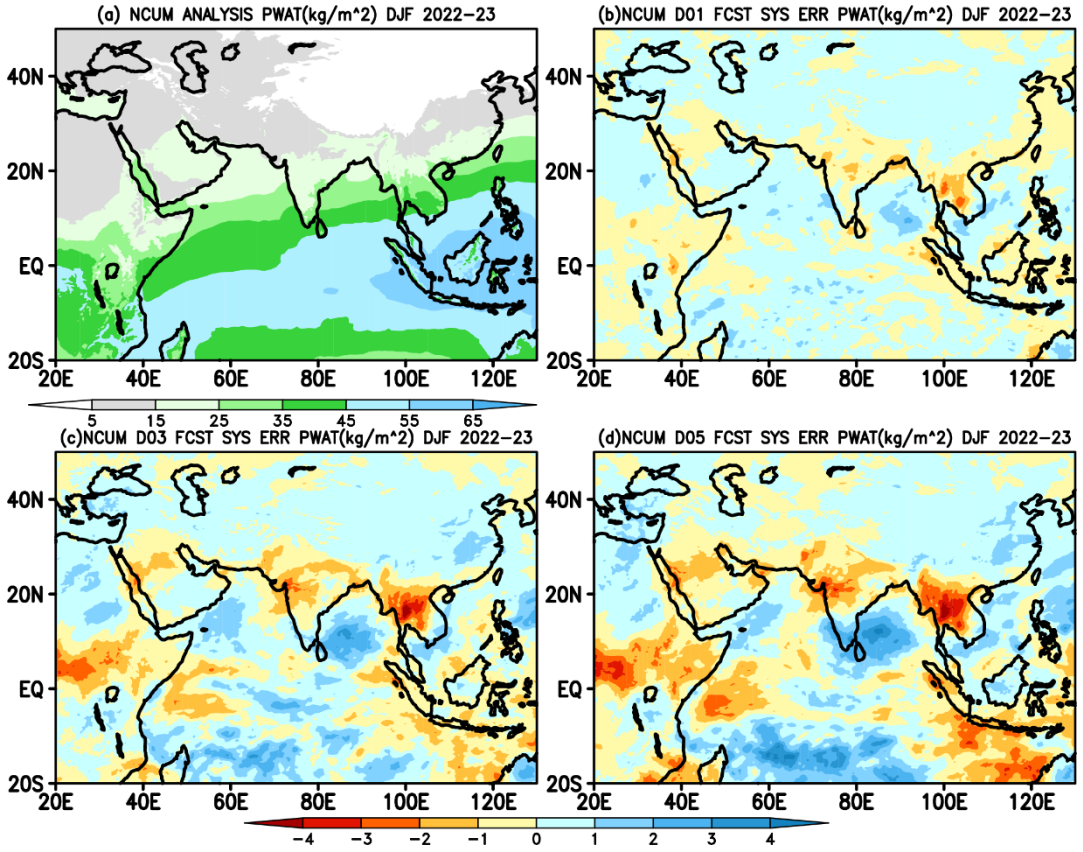

Figure 19. (a) Mean Total Precipitable Water (PWAT) up to model levels and systematic errors (mm) in (b) Day-1, (c) Day-3, and (d) Day-5 forecasts during DJF 2022-23.

5. Forecast Verification during DJF 2022-23

Verification of NCUM-G model rainfall forecasts is presented in this section for DJF 2022-23. The daily accumulated rainfall forecasts are verified against the NCMRWF-IMD merged Satellite and gauge rainfall product. The discussion presented in this section is confined to mean and mean error (ME) over the India region. Further, this section also quantifies forecast skill using standard verification metrics, namely, the probability of detection (POD), false alarm ratio (FAR), and critical success index (CSI) which are described in standard literature (Wilks, 2011, Jolliffe and Stephenson, 2012); and Symmetric extremal dependence index

(SEDI), a metric for extreme and rare events (Stephenson et al 2008, Ashrit et al 2015b, Sharma et al 2021).

5.1. Rainfall Mean and Mean Error

The observed and forecast mean rainfall during DJF 2022-23 is shown in Figure 20. Observations indicate the highest mean rainfall exceeding 10 mm/day is seen over the southern parts of peninsular India and equatorial oceanic regions. Moderate rainfall (2-4 mm/day) is seen over the Jammu and Kashmir (J & K) region where the effect of western disturbances is more prominent which brings a significant amount of rain occur over these regions (Figure 20a). The panels in the middle row, Figures 20 b-d show the Day-1, Day-3, and Day-5 NCUM-G forecast rainfall averaged during the DJF 2022-23 period. The observed peak in rainfall amount is well predicted in all the forecast lead times. However, it is found that the NCUM-G forecast overestimates rainfall amounts and spatial distribution over oceanic regions around the equator, north-eastern regions, and J & K regions. Apart from this most of the Indian subcontinent is dry with no convection in both observations and forecasts. Now, to further quantification forecast mean errors (ME) are computed against the observations. The panels in the bottom row show rainfall mean error (ME) (Figures 20 e-g) in predicted rainfall indicating wet bias (blue) over southern parts of the oceanic regions consistent with the mean rainfall patterns (Figures 20 b-d). Small dry bias regions are noticed over Sri Lanka, western parts of south BoB, and some parts of Tamil Nadu in the rainfall forecasts and the magnitude of dry bias increases with lead time (Figures 20 e-g).

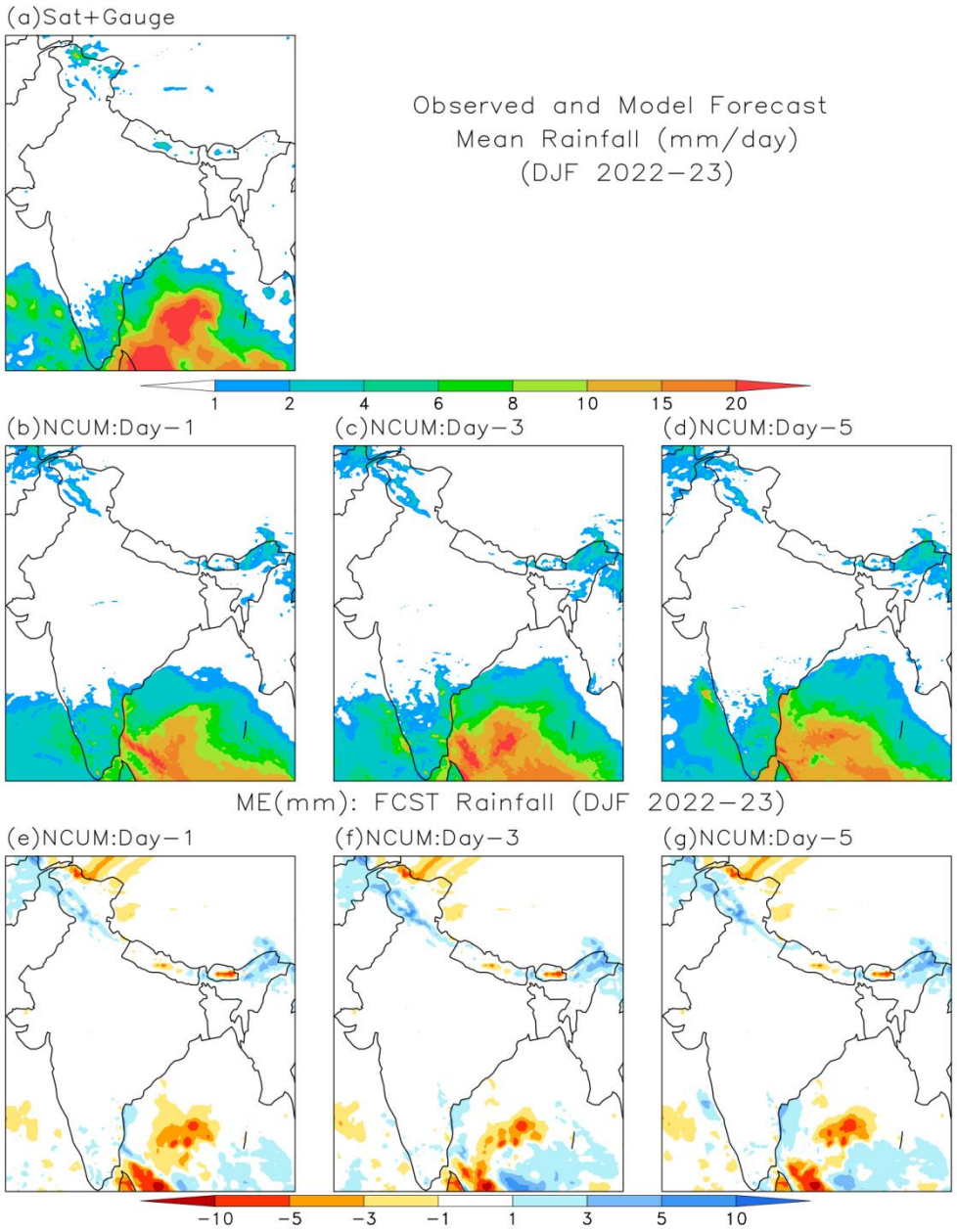

Figure 20. Accumulated DJF rainfall (mm) in (a) Observations and (b) Day-1, (c) Day-3, and (d) Day-5 forecasts. Bottom panels (e), (f), and (g) show Mean Error (ME) in Day-1, Day-3, and Day-5 forecasts, respectively.

5.2. Categorical Scores of Rainfall Forecasts

To further quantify the model rainfall forecasts, categorical skill scores are computed over the Indian subcontinent (Figure 21). The categorical approach of verifying quantitative precipitation forecast (QPF) is generally based on the 2 x 2 contingency table which is

evaluated for each threshold. Verification scores are presented for rainfall of up to 30mm/day. For different rainfall thresholds, POD and FAR show a decrease and increase in scores, respectively. The BIAS score (frequency bias) indicates that forecasts overestimate the frequency at various thresholds. The values of Peirce's skill score (PSS) and SEDI, all are high for rainfall up to 3-5 mm/day suggesting reasonable skill. PSS score shows a very sharp decrease as the threshold varies. Overall, the skill is not bias-free. For higher rainfall thresholds (> 10 mm/day), frequency bias is almost constant, but the skill is low as indicated by CSI, PSS, and SEDI (Figure 21).

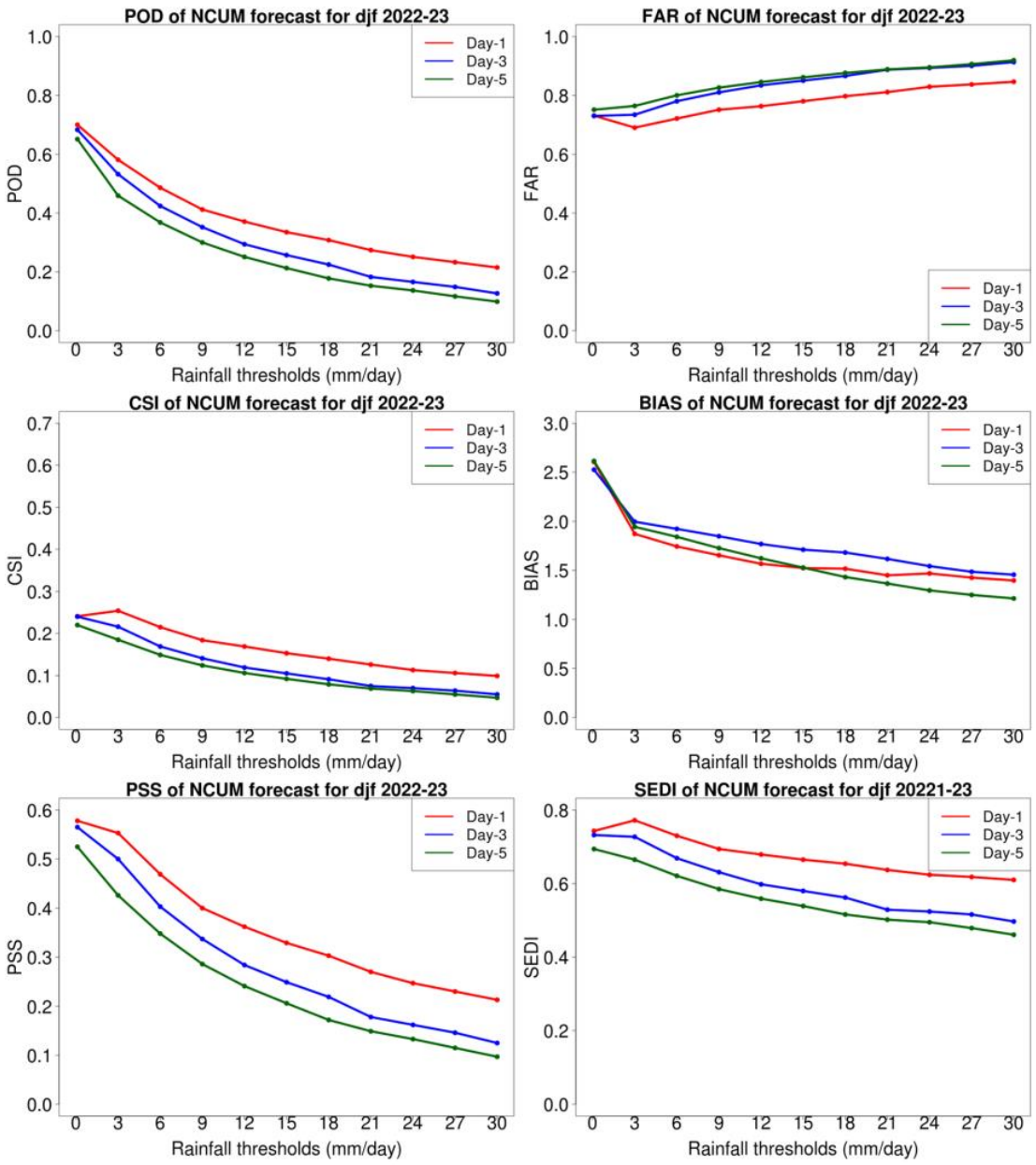

Figure 21. Categorical all India Rainfall scores POD (*top left*), FAR (*top right*), CSI (*middle left*), BIAS (*middle right*), PSS (*bottom left*), and SEDI (*bottom right*).

5.3. Categorical Scores of T_{min}

Similar analysis as discussed in above section 5.2 is repeated for minimum temperature (T_{min}) thresholds. Interestingly the POD and PSS scores for Tmin thresholds remain nearly constant up to 20-22^{0}C with values less than 0.4. However, the PSS scores slightly increase at 22-24^{0}C

(Figure 22). FAR scores over India as a whole show relatively large values >0.6 up to temperature thresholds 18-20^{0}C, later a gradual decrease is noticed in all the forecast times (Figure 22).

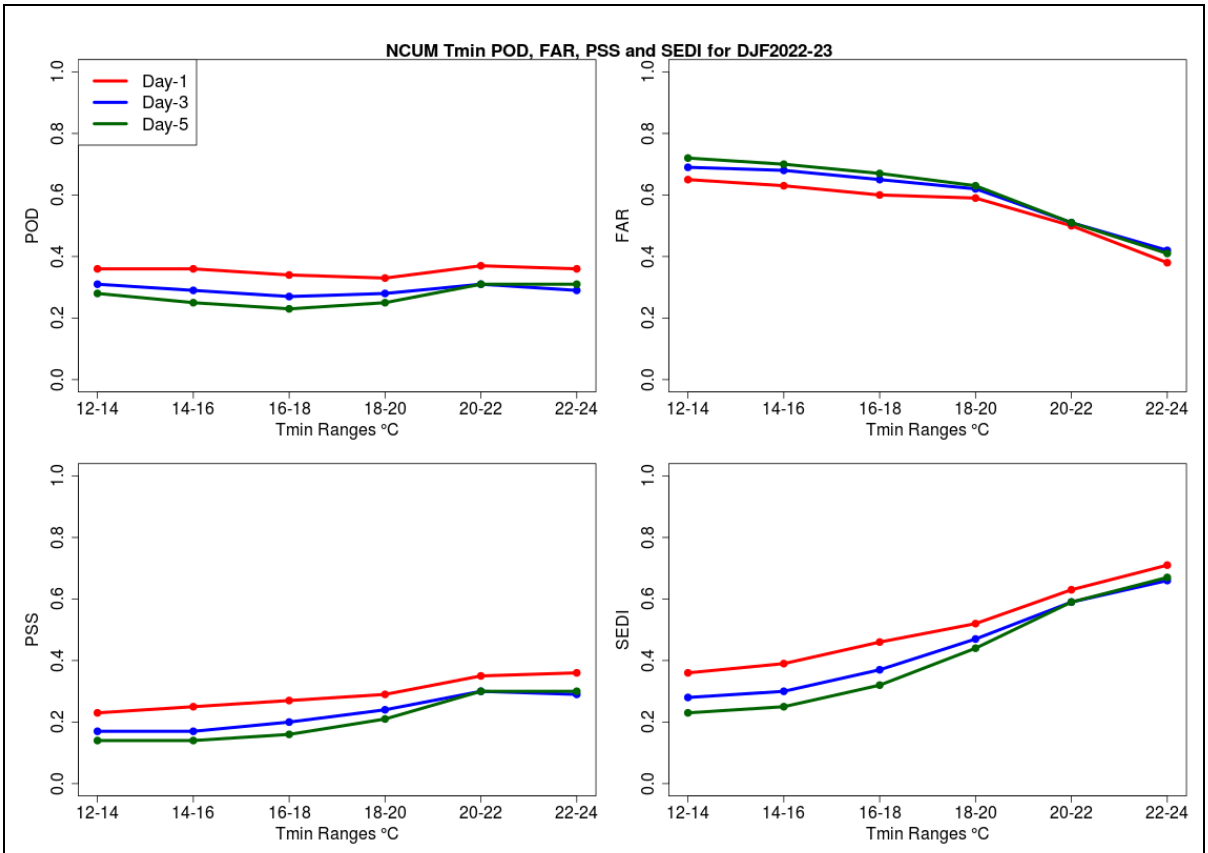

Figure 22. Categorical all India T_{min} scores POD (*top left*), FAR (*top right*), PSS (*bottom left*), and SEDI (*bottom right*).

6. Significant Weather Events during DJF 2022-23

This section summarizes the significant weather events such as the cyclones, western disturbances, cold waves, extreme rainfall events, etc., that happened during the DJF 2022 – 23season along with the forecast assessment from the NCUM-G model.

6.1. Bay of Bengal SCS "Mandous" during 06-10 Dec 2022

This section gives a summary report on the verification of the NCMRWF model forecasts for the recent Severe Cyclonic Storm (SCS) 'MANDOUS' during 06-10 Dec 2022, which developed over the Bay of Bengal (BoB) and crossed the Tamil Nadu coast during the early

hours on 10th Dec 2022. Verification of forecast tracks and intensity is presented for all NCMRWF Unified Models; NCUM-G (12 km grid resolution), NCMRWF Global Ensemble Prediction System (NEPS-G; 12 km grid resolution), NCMRWF Regional Unified Model (NCUM-R; 4 km grid resolution) for both 00UTC and 12UTC runs; and NCMRWF Regional Ensemble Prediction System (NEPS-R; 4 km grid resolution) for 00UTC runs. Forecast tracks and verification is presented for model-predicted tracks against IMD best track data. Appendix-1 gives details of all NCMRWF models and forecasts used for tropical cyclone forecasting. A brief description of cyclone tracker operationally used is also given in Appendix-1.

6.1.1. Forecast Tracks and Strike Probability

The observed and predicted tracks based on 00UTC of 8th Dec 2022 are shown in Figure 23 (top). All the predicted tracks indicated that the SCS "Mandous" would track towards Tamil Nadu and make landfall near Puducherry. The strike probability (Figure 23; bottom) based on the 22-member NEPS-G ensemble indicate that the cyclone would approach the northern Tamil Nadu coast in forecast based on 8th Dec 2022. The forecast track errors are discussed in the next section.

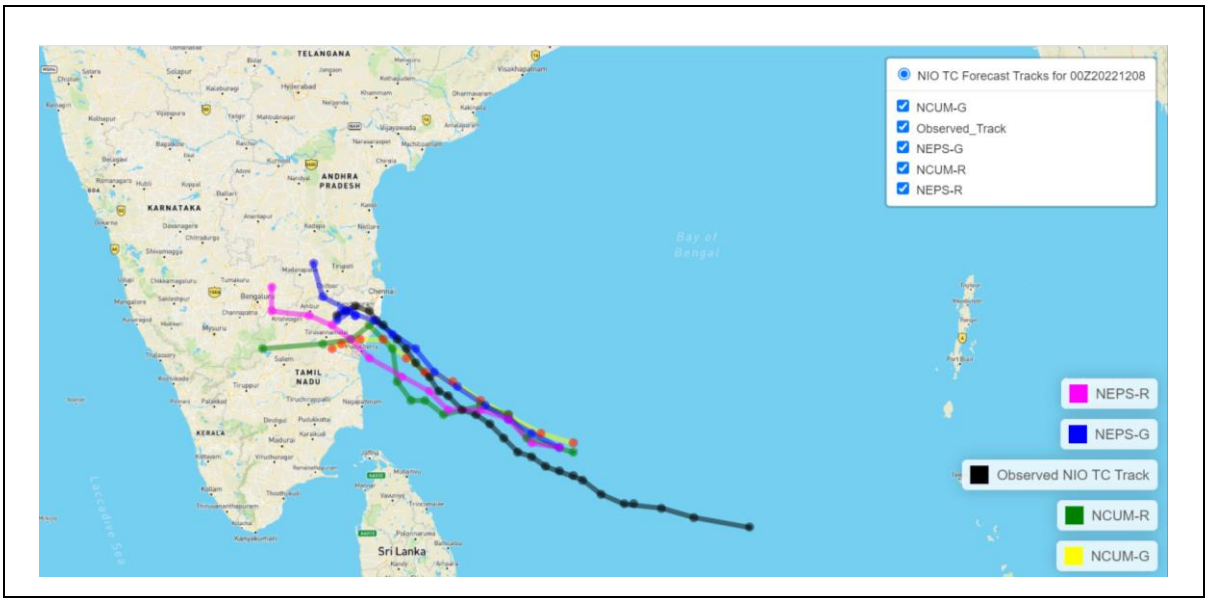

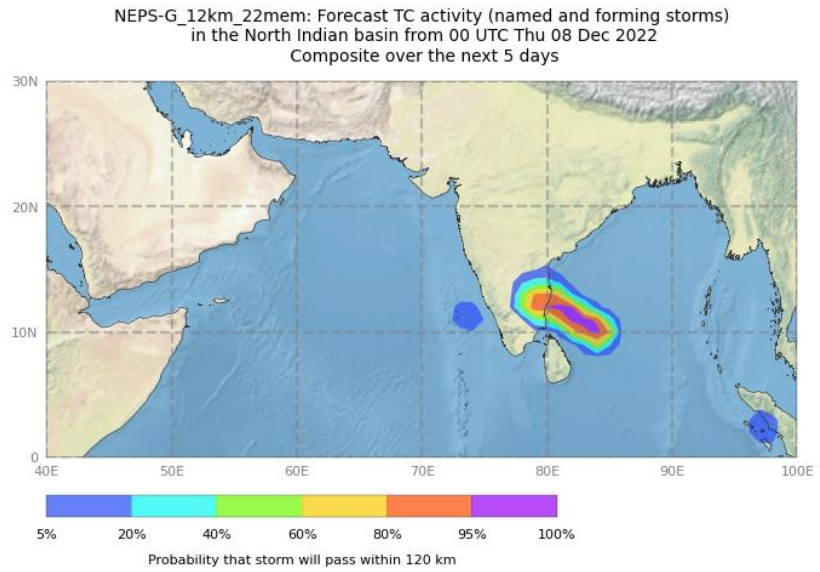

Figure 23. Observed & forecast tracks of Bay of Bengal SCS 'Mandous'. Forecast tracks, strike probability, and EPS grams are based on IC 00UTC 8th Dec 2022.

6.1.2. Forecast Track Errors

The NCUM-G (ICs from 3-9 Dec 2022), NEPS-G (ICs 6-9 Dec 2022), and NCUM-R (ICs from 4-9 Dec 2022) tracks based on 00UTC and 12UTC runs, and NEPS-R (ICs 6-10 Dec 2022) tracks based on 00UTC runs have been used in the verification. Table 1 summarizes the track errors at different lead times. Mean initial position error is the least (35 & 39 km) in NEPS-G & NEPS-R. NEPS-G (ensemble mean) demonstrates the lowest Direct Position Error (DPE) for the first 96hrs. Furthermore, both Global models (NCUM-G and NEPS-G) have DPE < 100 km for the initial 48hrs.

The track error components of Direct Position Error (DPE), Along Track Error (ATE), and Cross Track Error (CTE) are shown in Figure 24. DPE & ATE are highest in NCUM-R up to 72hrs. High DPE in NCUM-R and NEPS-R (after 48hrs) is mainly contributed by high CTE.

Table 1. Forecast Track Errors NCUM-R, NCUM-G, NEPS-R, and NEPS-G (numbers in the adjacent column in italics indicate number of forecast points validated)

	DPE							
Fcst Hour	**NCUM-R**	**No of Fcst verified**	**NCUM-G**	**No of Fcst verified**	**NEPS-R**		**NEPS-G**	**No. of Fcst verified**
0	67	*6*	58	*6*	39	4	35	*7*
12	72	*7*	48	*7*	46	4	49	*8*
24	81	*7*	60	*6*	61	4	50	*7*
36	115	*7*	68	*7*	65	3	52	*6*
48	144	*7*	91	*7*	133	3	67	*5*
60	163	*7*	129	*8*	184	2	83	*4*
72	191	*6*	146	*8*	236	2	78	*3*
84			181	*8*			62	*2*
96			210	*7*			86	*1*
108			245	*5*			NA	*0*
120			219	*4*			NA	*0*

(a)

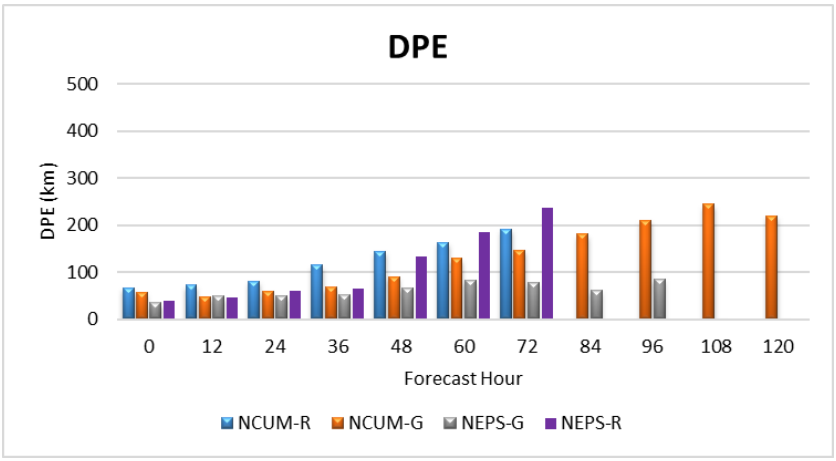

(b)

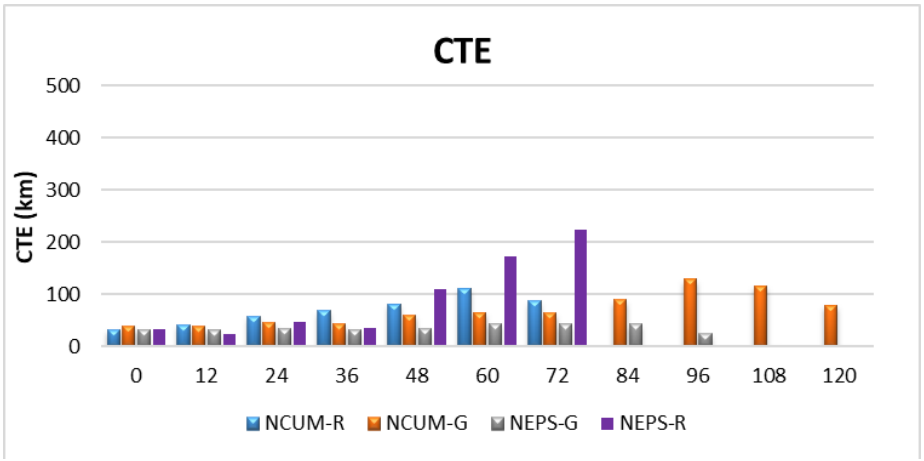

(c)

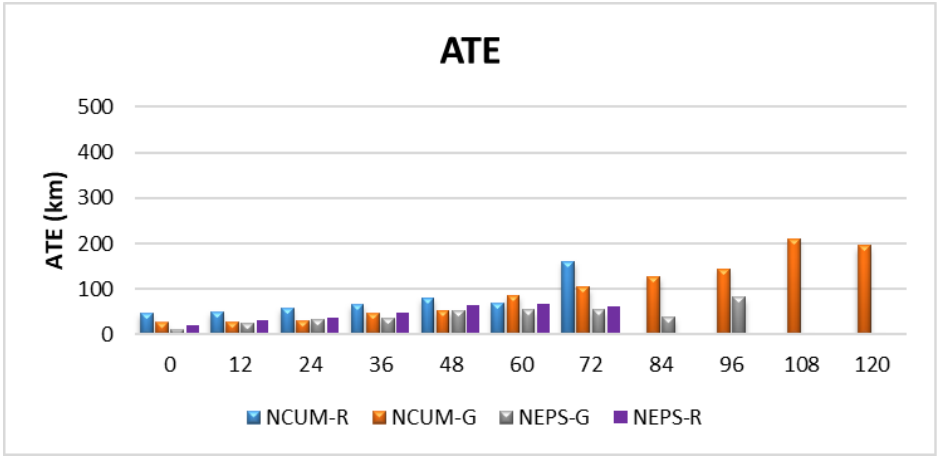

Figure 24. Track forecast errors (a) Direct Position Error (DPE), (b) Along Track Error (ATE), and (c) Cross Track Error (CTE) in km.

6.1.3. Forecast Intensity errors (Min SLP and Max Wind)

The mean absolute error (MAE) in forecast central pressure (CP)/minimum Sea level Pressure (Min SLP) and maximum sustained wind (MSW) for NCUM-R and NCUM-G models is shown in Figure 25. Average error in MSW is low in NCUM-G. At the initial time, the MEA in CP (MSW) is < 3 hPa (20 kt) in both NCUM-G & NCUM-R. The magnitude of MSW is higher (>10 kt) in NCUM-R and lower (<5 kt) in NCUM-G up to 72hrs. This is also reflected in Figure 26 where the NCUM-G forecasts have very realistic representation of MSW and Min SLP with different ICs.

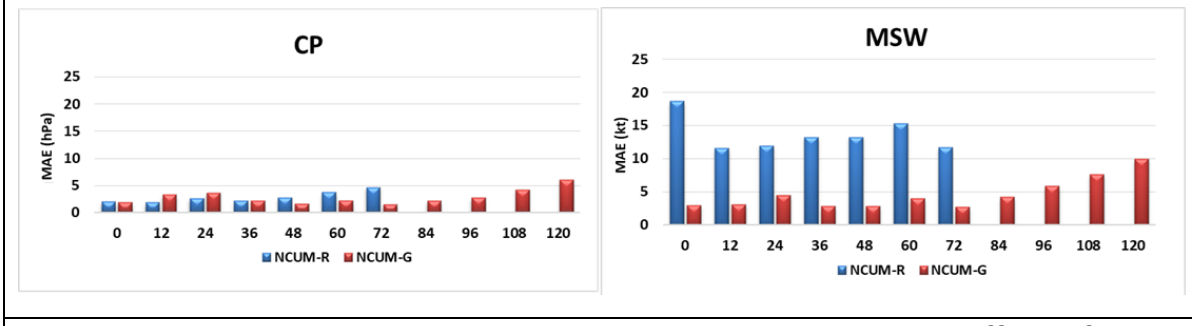

Figure 25. Mean Absolute Error (MEA) in CP (hPa) and MSW (kt) at different forecast lead times.

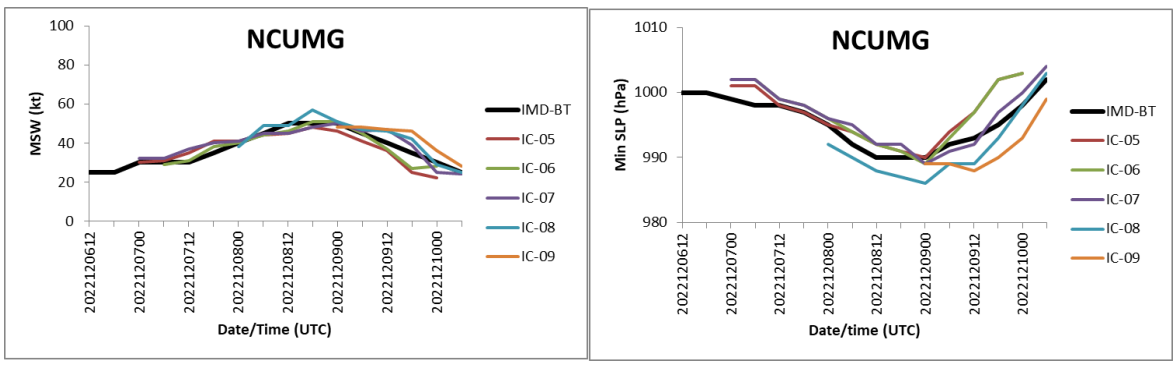

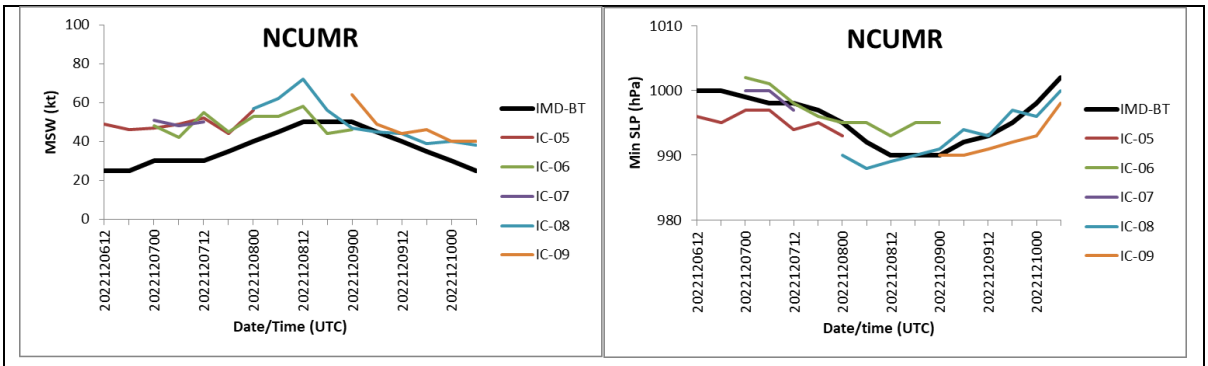

Figure 26. Intensity given by MSW (left) & Min SLP (right) in NCUM-G (top) and NCUM-R (bottom) forecasts with different initial conditions from 5th – 9th Dec 2022.

6.1.4. Forecast Landfall Error

As per the IMDs best track data the SCS "Mandous" landfall time is 18-20 UTC on 9th Dec and the position is 12.6 ^{0}N and 80.5 ^{0}E. The forecast landfall errors have been computed using the first forecast position on the land. *The forecast landfall time error is +5 hours in all models from 12UTC 08 Dec onwards. The best forecast in terms of landfall time was on 7th Dec 2022 where both 00 and 12UTC runs showed -1hr* (although large distance error in forecast position of landfall).

Table 2. Error in the forecast landfall time and position (Forecast time – Observed time) [-ve depicts early landfall and +ve shows delay in landfall]

	NCUM-G		NEPS-G		NCUM-R		NEPS-R	
	Time Error	**Distance Error**	**Time Error**	**Distance Error**	**Time Error**	**Distance Error**	**Time Error**	**Distance Error**
00Z06DEC2022	-07:00	67	17:00	28				
12Z06DEC2022	-01:00	98	5:00	62				
00Z07DEC2022	5:00	132	-01:00	185			-01:00	185
12Z07DEC2022	-01:00	107	-01:00	83	-01:00	161		
00Z08DEC2022	5:00	59	5:00	5	11:00	20	5:00	74
12Z08DEC2022	5:00	59	5:00	35	5:00	37		

00Z09DEC2022	5:00	59	5:00	29	5:00	82	5:00	54
12Z09DEC2022	5:00	68	5:00	54	5:00	117		

6.1.5. Verification of Strike Probability

Cyclone strike probability is the probability of locating a cyclone within 120km of any grid point (see Figure 24; bottom panel). Verification of strike probability is presented using Relative Operating Characteristics (ROC) and Reliability diagram (attributes diagrams). It must be noted that the verification of strike probability is presented for a common period from 5-10 Dec 2022. NEPS-R forecasts are available only for the 00UTC cycle and NEPS-G forecasts are available for 00 and 12 UTC runs. The sample sizes of both do not match and hence the results should be considered indicative and not accurate. The Reliability diagram gives a comparison of forecast probability against the observed frequencies. A perfect match will show all points along the diagonal line. Points above the diagonal suggest underestimation (lower forecast probabilities) while points below the diagonal suggest overestimation (higher forecast probabilities).

For the SCS "Mandous" case, the strike probability verification obtained from NEPS-G & NEPS-R is carried out using the best track data. Figure 27 shows the reliability and ROC plots for the strike probability verification. In the Reliability diagram, the points along the diagonal would indicate the best-performing model. While points below (*above*) would indicate over (*under*) estimation of cyclone strike probability. *The NCUM-G model is over-forecasting as the observed frequencies are lower than the forecast probabilities. On the other hand, NCUM-R is over-forecasting. The ROC curves of NCUM-G and NCUM-R show that the models have the skill* as the curves are away from the diagonal line of no resolution. The AROC (area under the ROC) is higher for NEPS-G (0.89) compared to NEPS-R (0.77).

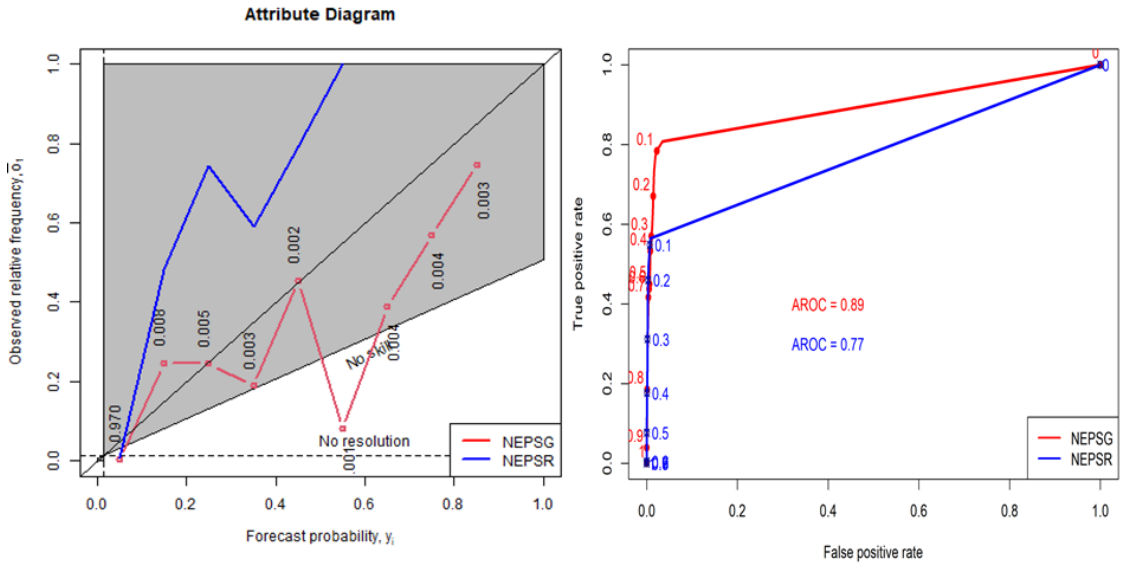

Figure 27. Verification of strike probability using reliability diagram (left) and ROC curve (right) for the case of SCS 'Mandous'.

6.1.6. CRA Verification of Rainfall Forecasts

Contiguous rain areas (CRA) verification is a spatial verification method (Ebert and Gallus 2009) that focuses on individual weather systems and verifies the properties of the forecast objects, which allows estimation of location error of the forecast entity. Detailed description of the method with application over India can be found for UM Rainfall forecasts over India (Ashrit et al 2015a) and MoES Models (NCUM & GFS) in Sharma et al., (2020). Here, NCUM-G rainfall forecasts corresponding to the SCS 'Mandous' on 8th and 11th Dec 2022 are discussed briefly using CRA verification (Figures 28 a-d). The results are presented for Day-3 (left panels) and Day-5 (right panels) forecasts valid on 8th Dec 2022 (top) and 11th Dec 2022 (bottom). On 8th Dec 2022, observed rainfall is mainly confined to Sea and away from the Indian coast. The forecasts underestimate the all attributes '*grid points>40mm*'(i.e., spatial coverage), '*Average Rainfall*', '*Maximum Rain*', and '*Rain volume*'. The forecast completely miss the observed rainfall over parts of Sri Lanka. In the Day-3 forecast, the 40mm/day object is shifted by 2.03° eastwards and 2.84° northwards. In the Day-5 forecast, the object is shifted by 0.50° eastwards and 3.55° northwards. Contribution to RMSE from pattern error is dominating (80.4% in Day-3 and 72.5% in Day-5 forecasts). On the other hand, the observed

rainfall on 11th Dec 2022 (Figures 28 c,d), covers parts of Andhra Pradesh, Tamil Nadu and Karnataka. The forecasts overestimate all the attributes. In this case the results are presented for 20mm/day CRA threshold. In the Day-3 forecast, the 20mm/day object is shifted by 1.28° eastwards and 0.77° northwards. In the Day-5 forecast, the object is shifted 2.00° eastwards and 0.82° northwards. The contribution to RMSE is again, mainly from the pattern error (86.1% in Day-3 and 83.6% in Day-5).

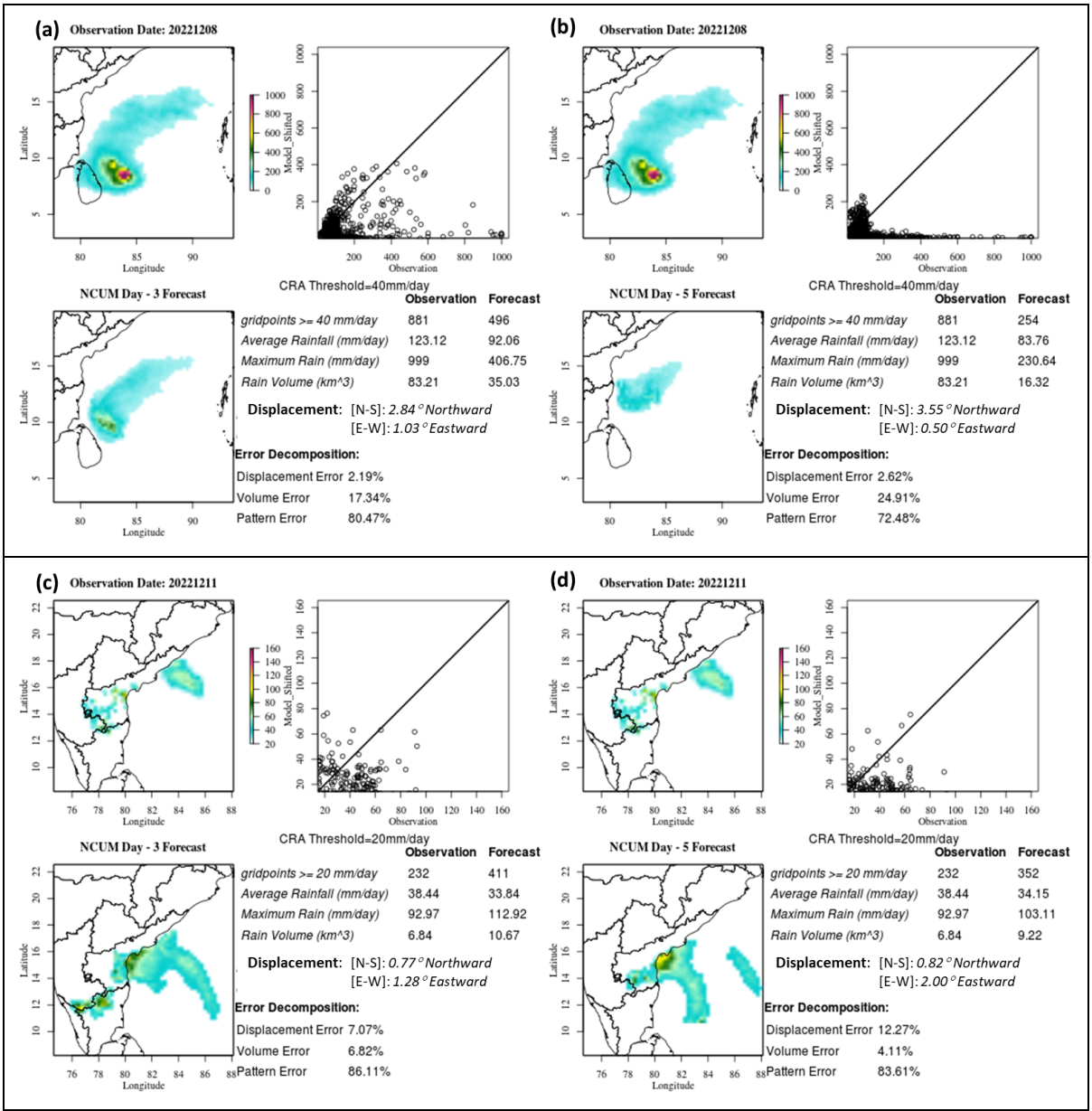

Figure 28 CRA verification of (a) Day-3 and (b) Day-5 rainfall forecasts valid on 8th Dec 2022 for 40 mm/day threshold. Similarly, CRA verification of (c) Day-3 and (d) Day-5 forecasts valid on 11th Dec 2022 is presented for 20 mm/day threshold.

6.2. Cold Waves & Western Disturbance

6.2.1. Verification of Tmin & Western disturbance

Figure 29 and 30 shows the observed and forecast minimum temperature on 06th Jan 2023 and 17th Jan 2023, respectively. A large part of north India shows Tmin lower than 10^{0}C in the observations which is accurately predicted in each of the forecasts. A minimum temperature < 4^{0}C is seen in the observations over northwest India (see Figure 29). The NCUM-G forecasts successfully predict the low Tmin values over northwest India. However, the model forecasts show low temperatures over a larger area. Similarly, Figure 30 shows the observed and forecast Tmin on 17th Jan 2023. The forecasts show a reasonable match with the observations. Out of all the western disturbances (WDs) during the winter season (DJF), 2022-2023 listed in Table 3, we have chosen the strongest WD case for this report. The NCUM-G model forecasts clearly indicate the location and intensity of the trough and WD formation as seen in observation (see Figure 31) and associated rainfall over northwestern India (see Figure 32).

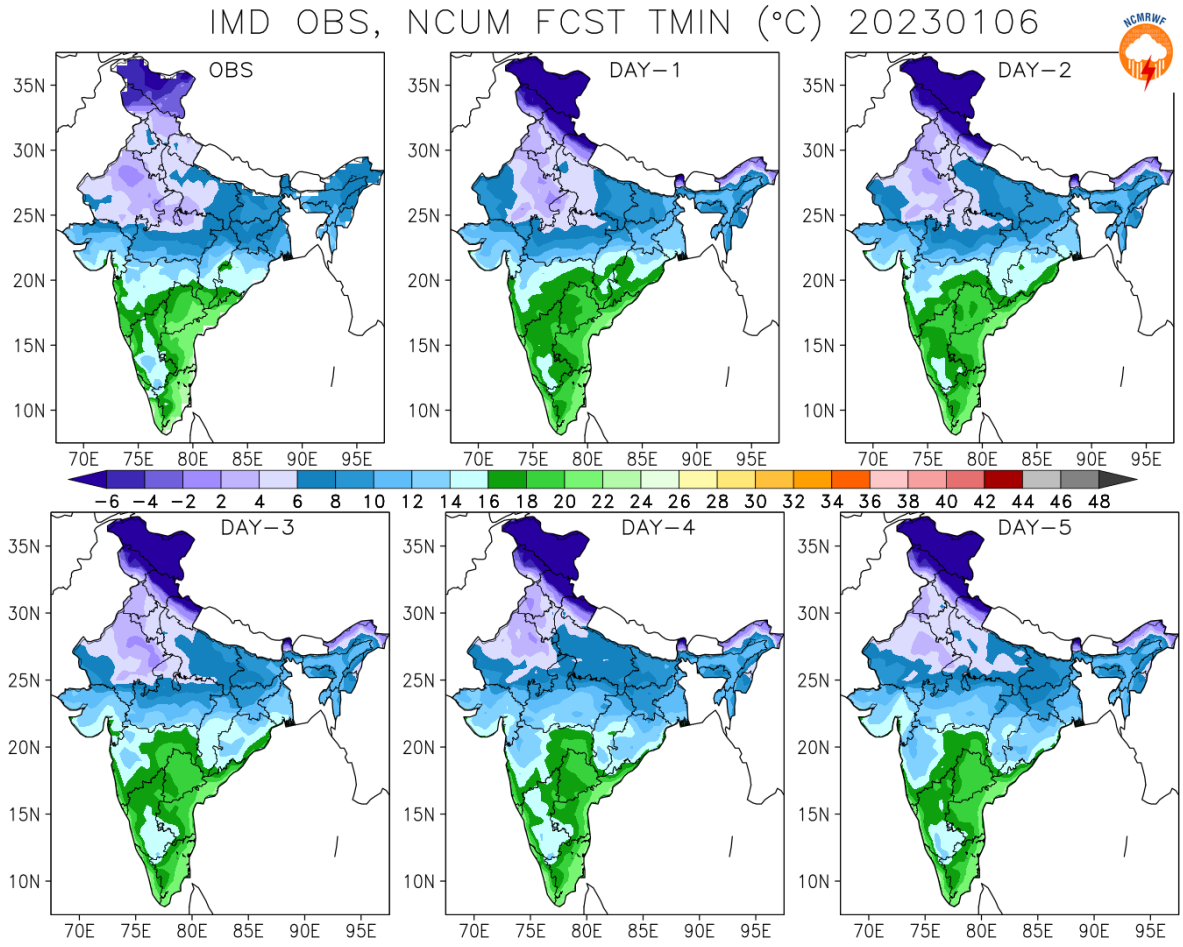

Figure 29. Observed and forecast Tmin valid on 06th Jan 2023 over India.

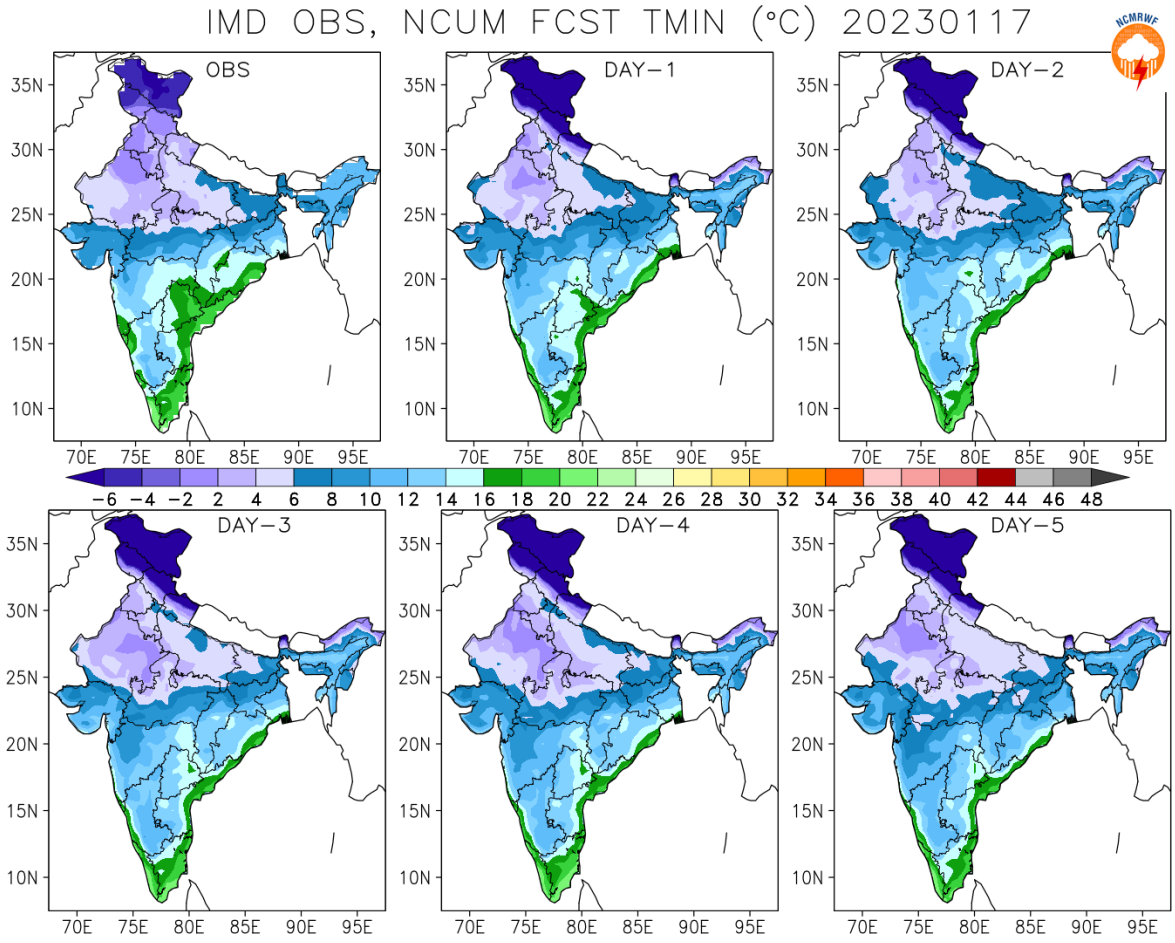

Figure 30. Observed and forecast Tmin valid on 17th Jan 2023 over India.

Table 3. List of DJF seasonal Western Disturbances.

S. No.	Month	Western Disturbances		
		Total	**Weak**	**Strong**
1.	December	**7**	**6** (i.e., 2-4 Dec, 6-8 Dec, 11-15 Dec, 17-21 Dec, and 22-24 Dec)	**1** (i.e., 28-30 Dec)
2.	January	**7**	**3** (i.e., 1-3, 3-5, 5-10 Jan)	**4** (i.e., 11-14 Jan, 18-21 Jan, 23-27 Jan, and 27-30 Jan)
3.	February	**5**	**5** (i.e., 1-5, 5-7, 8-12, 18-22, and 26-28 Feb)	**0**

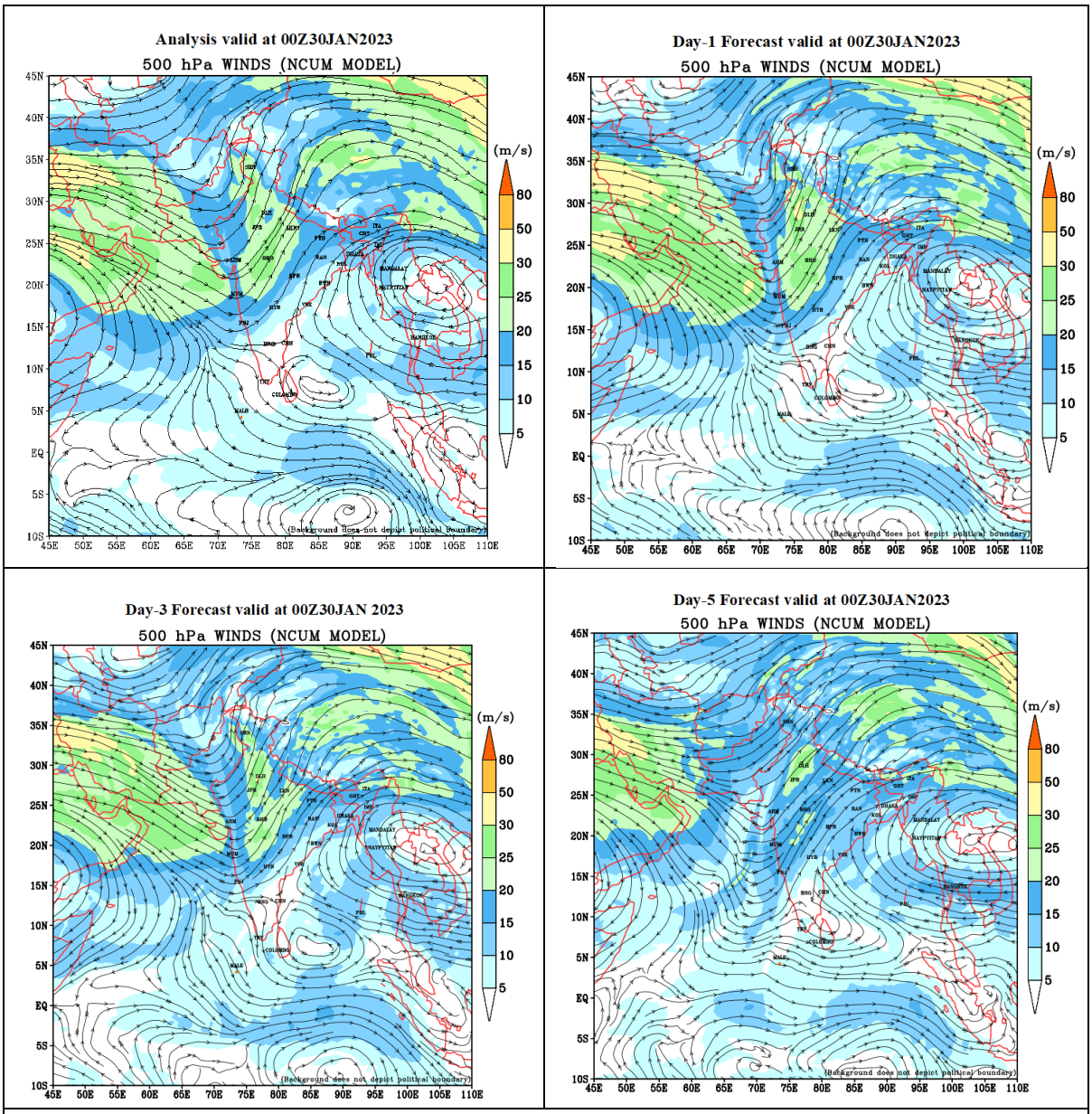

Figure 31. NCUM-G winds at 500 hPa in the analysis and Day-1, Day-3, and Day-5 forecasts valid on 30th Jan 2023

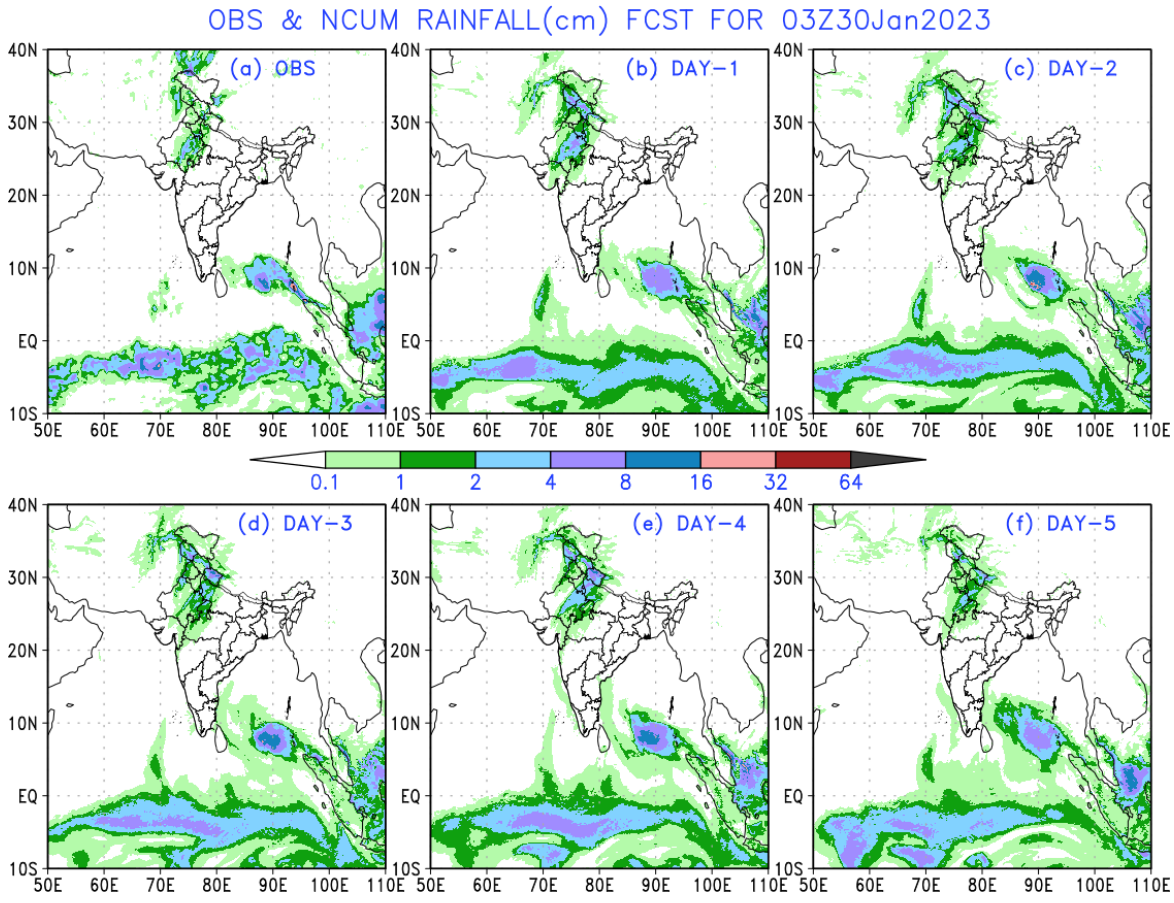

Figure 32. Observed and forecast Rainfall valid on 30th Jan 2023.

6.2.2. Observed and forecasted daily Tmin time series

Further, verification of the Tmin forecasts based on the NEPS-G ensemble is shown for several locations over northwestern India. Observed Tmin data is obtained from SYNOP stations over India via the GTS network. Figure 33 shows the forecasts with IC of 1st Jan 2023. The NEPS control (red), ensemble mean (blue), and ensemble members (green) are compared with the observations (black). Observed Tmin generally lies within the spread of ensemble members. Ensemble mean shows very good match with the observations and successfully predicts sharp rise/fall in value consistent with observations. The sharp drop in observed Tmin in Agra (Gwalior) by about 3ºC (3ºC) between 05-08 (03-04) Jan 2023 is accurately predicted. Similarly for another case of cold wave in January 2023 is shown in Figure 34 for IC of13th Jan 2023. Prolonged spell of low Tmin is indicated in the forecasts consistently. The sharp

drop in observed Tmin in Agra (Lucknow) by about 9^{0}C (5 ^{0}C) between 15- 17 (15-16) Jan 2023 is accurately predicted.

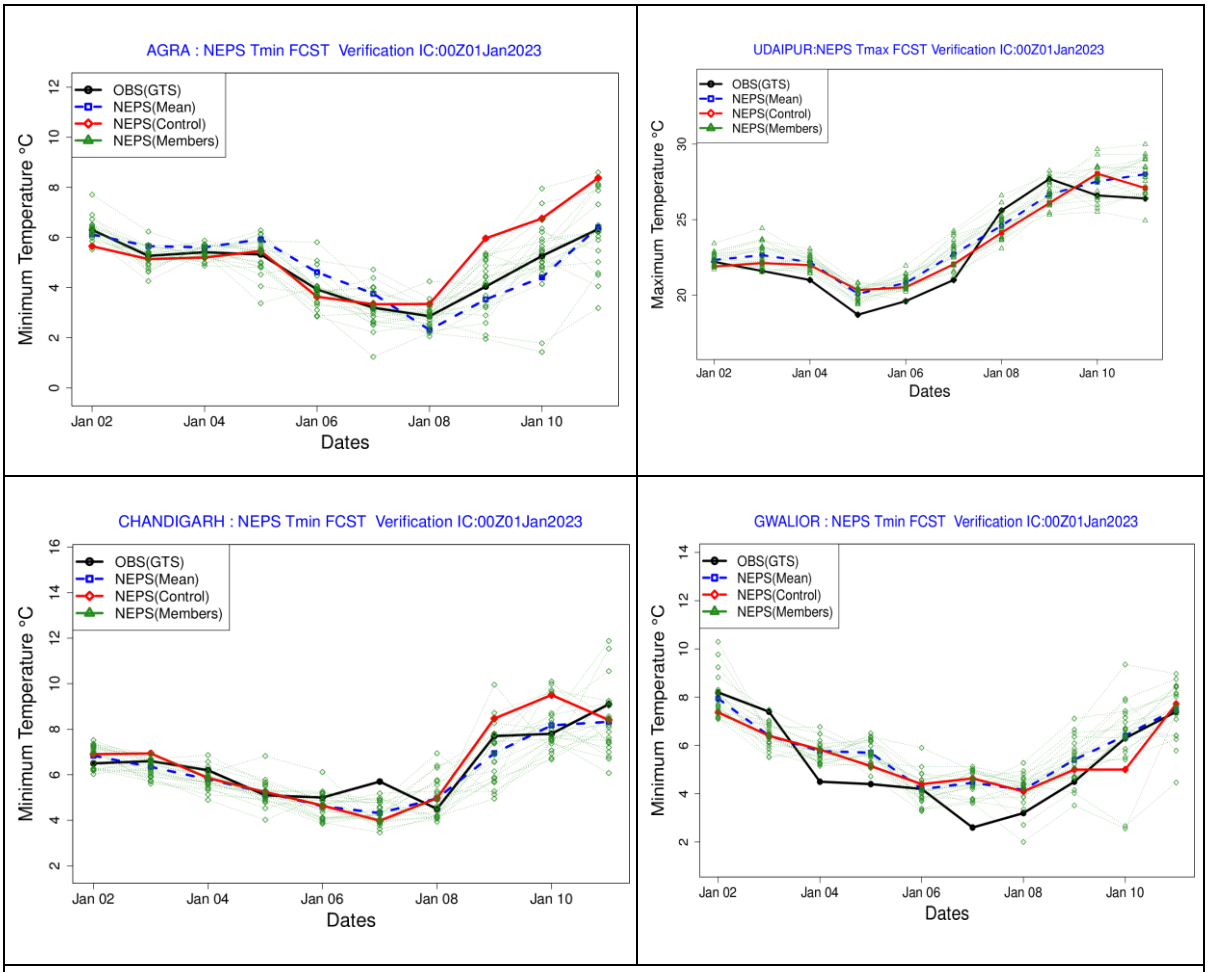

Figure 33. Observed and NEPS-G forecast Tmin over different cities over North India during the cold wave conditions of 1st Jan 2023.

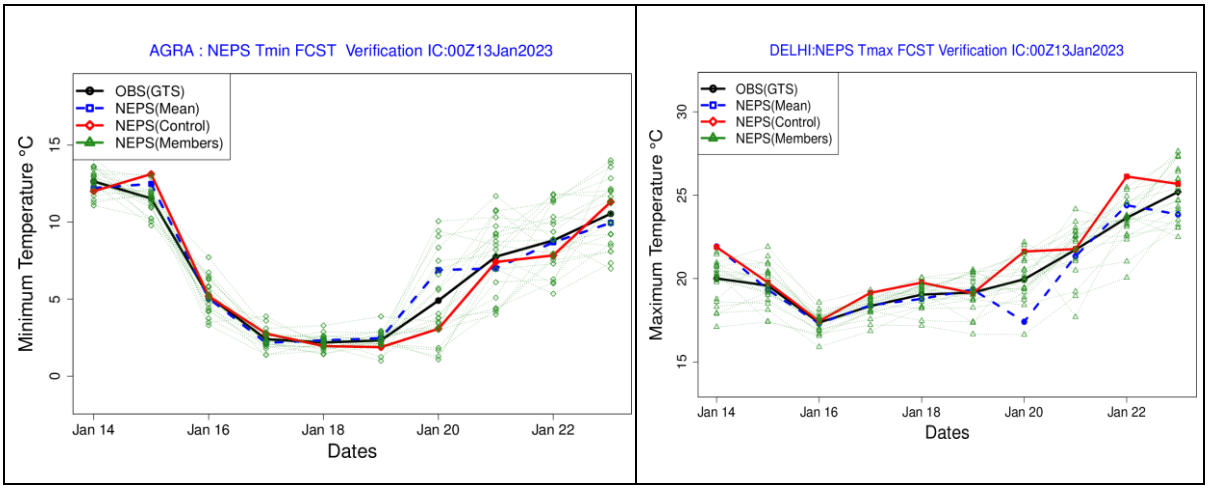

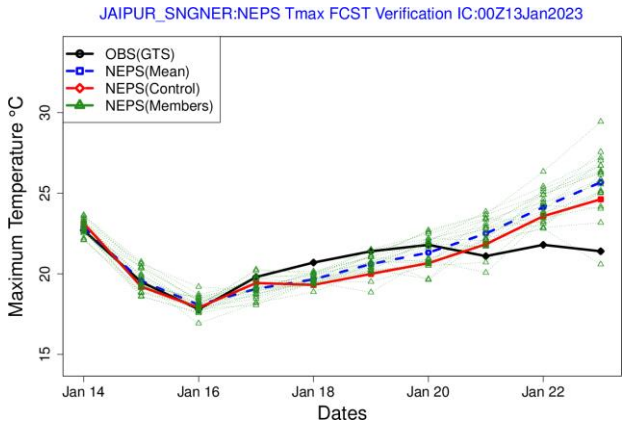

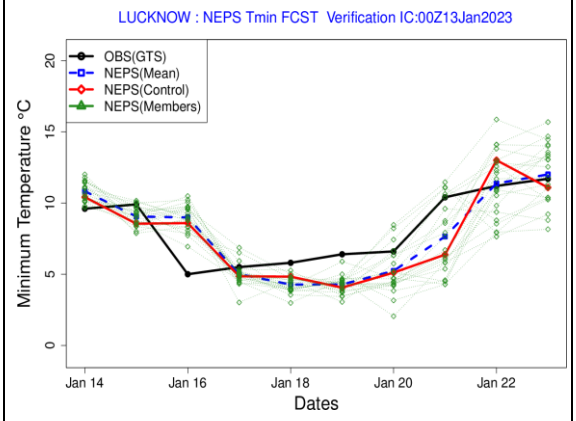

Figure 34. Observed and NEPS-G forecast Tmin over different cities over North India during the cold wave conditions of 13th Jan 2023.

7. Summary and Conclusions

This report documents the performance of the NCMRWF model forecasts during the winter season DJF 2022-23. The verification results are presented to address (a) forecasters and (b) model developers. The information on biases in the forecast winds, temperature humidity, rainfall, etc., is crucial for the forecasters to interpret the model guidance for forecasting. Additionally, information on recent improvements in the model skill adds to confidence in the model forecasts. The results of the study can be summarized below.

7.1. NCUM-G Mean analysis and anomalies during DJF 2022-23

- *The low-level wind anomalies at 850 and 700 hPa show the presence of anticyclonic circulation over the Central Indian region indicating high pressure and subdued convection. Penetrating westerlies from higher latitudes having relatively large magnitudes w.r.t ERA5 climatology towards the Indian subcontinent is evident. The anomalous easterlies are clearly discernible prevailing from the west Pacific to the Middle Eastern region in the upper troposphere over the north India. In the equatorial regions, the upper tropospheric winds are quite strong with magnitudes of more than 6m/s in winter 2022-23.*
- *Low level (850 and 700 hPa) temperature anomalies indicate the winter 2022-23 is warmer than the climatology with magnitudes between 1-2 ^0C in north India. The warmer temperatures stretch from northwest to southeast India covering the Indo-Gangetic plains.*

- *DJF 2022-23 indicates a lower percentage of RH compared to the climatology over the entire India land. The Oceanic regions of the Bay of Bengal and Arabian Sea also show positive anomalies in the humidity distribution for the winter period and negative anomalies are noted in the equatorial regions.*

7.2. NCUM-G Systematic Errors

- *Systematic errors in winds at 850 hPa from Day-1 forecasts show an easterly wind bias over the south Bay of Bengal. A westerly wind bias south of the equator around 60^0E and an easterly wind bias around the maritime continent (MC) is also noted. With forecast lead time these errors in low-level winds enhance and this could be due to the enhanced convective activity around the equatorial regions during the winter season. Westerly wind bias is more prominent at 700 hPa level over central India and the northeastern regions in Day-3 and Day-5 forecasts. Systematic errors at 200 hPa level winds show enhanced divergent circulation centered around central parts of India in Day-3 forecasts and similar spatial pattern in winds is also seen in Day-5 forecasts with enhanced error magnitudes.*
- *Model errors show warm bias (~1 ^{0}C) occupied over most of the Indian land mass, and this bias's magnitude is increasing with forecasts lead time. These error increments at 850 hPa temperatures are also more prominent over eastern African regions. On a similar note, temperature errors at 700 hPa also show warm bias (~0.5 ^{0}C) over the northern and central Indian regions. Interesting to see that the bias over BoB region reverse sign now exhibits warm bias compared to the 850hPa level. Systematic errors at 500 and 200 hPa levels show warm and cold bias, respectively, over the Indian land region including surrounding oceanic regions.*
- *Systematic errors in RH show a large dry bias over Indian land regions at 850 hPa level and the dryness is enhancing with forecasts lead time. The Omni presence of strong north easterlies over open oceanic regions of AS and BoB and increased evaporation could be one primary reason for the positive RH values over these regions. On the contrary, most of the Indian subcontinent and surrounding oceanic regions exhibit moist bias as evidenced by positive RH values, except Africa, the South China Sea, MC, and south of the equator regions. Interestingly the dry bias observed over the Indian land region at 850 hPa level change sign to positive and moist bias is seen at 700 hPa level. Additionally, the moist bias south of the equator is getting intensified in the Day-3 and Day-5 forecast and the entire column is occupied with excess moisture at 700 hPa levels.*
- *Systematic errors in surface winds at 10ml show North easterlies in Day-1 is changing its direction to southerlies with lead time and it is clearly seen on Day-5. The north-westerly wind bias over northern AS in Day-1 is enhancing its strength with forecasts lead time. On a similar note, the easterly wind bias seen in south of the equator around ~100 ^{0}E is also getting intensified with forecast lead time.*

- *Systematic errors in 2m temperature show a relatively warm bias over Indian land regions and north of 40 ^{0}N latitude regions. Interestingly these warm biases are increasing with forecast lead time, especially over the Indian region. This can be attributed to the dry north-westerly winds from the Northwest entering into Indian land and North AS. In addition, most of the oceanic regions of the BoB and AS exhibited warm bias of the range 0-0.5 ^{0}C in all the forecast lead times.*
- *Systematic error in PWAT shows a column dry over the northern and central Indian regions on Day-1, this dryness in the column is enhancing with forecast lead time, and its magnitude is maximum in Day-5. Large positive PWAT biases are seen over BoB, AS, and over equatorial regions. This excess column water could be one reason for excess rainfall over these regions.*

7.3. Forecast Verification during DJF 2022-23

- *NCUM-G forecast overestimates rainfall amounts and spatial distribution over oceanic regions around the equator, northeast, and J & K regions. Rainfall means error (ME) show wet bias over southern parts of the oceanic regions consistent with the mean rainfall patterns. Small dry bias regions are noticed over Sri Lanka, western parts of south BoB, and some parts of Tamil Nadu in the forecasts and the magnitude of dry bias increases with lead time.*
- *For different rainfall thresholds (3-30mm/day), POD and FAR show a decrease and increase in scores, respectively. POD >= 0.4 for rainfall up to 6 mm/day. The BIAS score (frequency bias) indicates that forecasts overestimate the frequency all thresholds. The values of PSS and SEDI all are high for rainfall up to 3-5 mm/day suggesting reasonable skill. PSS score shows a very sharp decrease as the threshold varies. Overall, the skill is not bias-free. For higher rainfall thresholds (> 10 mm/day), frequency bias is almost constant, but the skill is low as indicated by CSI, PSS, and SEDI.*
- *Interestingly the POD and PSS scores for Tmin thresholds remains nearly constant up to 20-22 ^{0}C with values less than 0.4. However, the PSS scores slightly increase at rainfall 22-24 ^{0}C. FAR scores over India as whole shows relatively large values >0.6 up to temperature thresholds 18-20 ^{0}C, later a gradual decrease is noticed in all the forecast times.*

7.4. Verification for Significant Weather Events during DJF 2022-23

Bay of Bengal SCS 'Mandous' (06-10 Dec 2022), Western Disturbances, extreme rainfall events, and Cold waves formed significant weather events of DJF 2022-23.

- ***Early Tracks****: NCUM-G starts tracking the system since 3rd Dec showing its intensification and movement towards Tamil Nadu coast. Forecast tracks based on 00UTC of 5th Dec show its landfall over Tamil Nadu coast. These early tracks do not show re-curvature over the Sea.*
- ***Initial Position Erro****r: Mean initial position errors are lower in NEPS-G (35 km) & NEPS-R (39 km).*
- ***Direct Position Erro****r: NCUM-G and NEPS-G show track errors less than 100 km up to 48 hrs. The mean DPE in NEPS-G is less than 100 km up to 96 hrs. At 96- and 120-hrs direct position error in NCUM-G is 210 and 219 km.*
- ***Landfall Position & Time error****: The landfall position errors <55 km are from 00Z08 (42 hrs in advance) in NEPS-G with the lowest error on 8th Dec. Landfall time errors in all the models are < 6 hr (delayed) since 8th Dec except NCUM-R on 00Z08 Dec. The best forecast in terms of landfall time was on 7th Dec 2022 where both 00 and 12UTC runs showed -1hr (early).*
- ***Intensity verification (NCUM-G & NCUM-R)****: MAE in both CP and MSW is higher in NCUM-R (overestimation of intensity) up to 72 hrs. NCUM-G shows an average error in CP and MSW less than 6 hPa and 10 kt at all the lead times.*
- ***Verification of strike probability (NEPS-G & NEPS-R)****: ROC and Reliability diagrams are used for this purpose. The NCUM-G model is over forecasting whereas NCUM-R is over-forecasting. The ROC curves show that the models have reasonable skill (ROC is 0.89 and 0.77 for NEPS-G and NEPS-R).*
- ***The spatial verification*** *of Day-3 & Day-5 rainfall valid on 8th and 11th Dec 2022 corresponding to SCS 'Mandous' consistently indicate eastward and northward shift in forecasts. While the object parameters (area, mean rainfall, highest amount and volume) for 40mm/day threshold (over sea) suggest forecasts underestimate, for 20mm/day CRA (over land) the forecasts underestimate. The forecast error is mainly contributed (>70%) by the pattern error.*
- *For the* ***Western Disturbance****, the forecast shows an accurate prediction of the trough in the westerlies at 500 hPa up to 5 days ahead. Associated low temperatures are accurately predicted in the NEPS-G ensemble mean. Ensemble members have a reasonable spread around the observations indicating reliability in ensemble forecasts.*

References

1. Ashrit, R., Elizabeth Ebert, Ashis K. Mitra, Kuldeep Sharma, Gopal Iyengar and E.N. Rajagopal 2015a: Verification of Met Office Unified Model (UM) quantitative precipitation forecasts during the Indian Monsoon using the Contiguous Rain Area (CRA) method. NMRF/RR/03/2015.
2. Ashrit R, Sharma K, Dube A, Iyengar G R, Mitra A K and Rajagopal E N 2015b: Verification of short-range forecasts of extreme rainfall during monsoon; Mausam 66 375–386, 607.
3. Barker, D., 2011. Data assimilation-progress and plans, MOSAC-16, 9-11 November 2011, Paper16.6.
4. Ebert, E.E. and W.A. Gallus, 2009: Toward better understanding of the contiguous rain area (CRA) method for spatial forecast verification. Wea. Forecasting, 24, 1401-1415.
5. Hersbach H, Bell B, Berrisford P, et al. 2020: The ERA5 global reanalysis. Q J R Meteorol Soc. 2020;146:1999–2049. https://doi.org/10.1002/qj.3803
6. Jolliffe, I. T., and D. Stephenson, 2012: Forecast Verification: A Practitioner's Guide in Atmospheric Science, John Wiley & Sons, Ltd.
7. Kumar Sumit, A. Jayakumar, M. T. Bushair, Buddhi Prakash J., Gibies George, Abhishek Lodh, S. Indira Rani, Saji Mohandas, John P. George and E. N. Rajagopal 2018: Implementation of New High Resolution NCUM Analysis-Forecast System in Mihir HPCS. NMRF/TR/01/2019, 17p.
8. Kumar Sumit, Gibies George, Buddhi Prakash J., M. T. Bushair, S. Indira Rani and John P. George 2021: NCUM Global DA System: Highlights of the 2021 upgrade, NMRF/TR/05/2021.
9. Kumar Sumit, M. T. Bushair, Buddhi Prakash J., Abhishek Lodh, Priti Sharma, Gibies George, S. Indira Rani, John P. George, A. Jayakumar, Saji Mohandas, Sushant Kumar, Kuldeep Sharma, S. Karunasagar, and E. N. Rajagopal 2020: NCUM Global NWP System: Version 6 (NCUM-G:V6), NMRF/TR/06/2020
10. Mitra, A. K., A. K. Bohra, M. N. Rajeevan and T. N. Krishnamurti, 2009: Daily Indian precipitation analyses formed from a merged of rain-gauge with TRMM TMPA satellite derived rainfall estimates, J. of Met. Soc. of Japan, 87A, 265-279.
11. Mitra, A. K., I. M. Momin, E. N. Rajagopal, S. Basu, M. N. Rajeevan and T. N. Krishnamurti, 2013, Gridded Daily Indian Monsoon Rainfall for 14 Seasons: Merged TRMM and IMD Gauge Analyzed Values, J. of Earth System Science, 122(5), 1173-1182.
12. Sharma K., S. Karunasagar and Raghavendra Ashrit 2020: CRA Verification of GFS and NCUM Rainfall Forecasts for Depression cases during JJAS 2018. /NMRF/RR/05/2020
13. Sharma, K., Ashrit, R., Kumar, S. et al. Unified model rainfall forecasts over India during 2007–2018: Evaluating extreme rains over hilly regions. J Earth Syst Sci 130, 82 (2021). https://doi.org/10.1007/s12040-021-01595-1
14. Srivastava A K, Rajeevan M and Kshirsagar S R 2009: Development of a high resolution daily gridded temperature data set (1969–2005) for the Indian region; Atmos. Sci. Lett. 10 249–254, https://doi.org/10.1002/asl.232
15. Stephenson D.B., B. Casati, C.A.T. Ferro and C.A. Wilson, 2008: The extreme dependency score: a non-vanishing measure for forecasts of rare events. Meteorol. Appl., 15, 41-50.
16. Walters, D., and co-authors: The Met Office Unified Model Global Atmosphere 6.0/6.1 and JULES Global Land 6.0/6.1 configurations, Geosci. Model Dev., 10, 1487–1520, https://doi.org/10.5194/gmd-10-1487-2017, 2017
17. Wilks D S 2011 (eds) Statistical methods in the atmospheric 807 sciences; 3rd edn, Elsevier, 676p

Appendix-I

A1. Brief Description of NCMRWF Models and the new TC tracker

(i) NCMRWF Unified Model (NCUM-G, NCUM-R, NEPS-G and NEPS-R)

Table-A1: NCMRWF Unified Model configuration

Model	Application & Domain	Resolution	Forecasts	Track Prediction
NCUM-G	Global NWP Forecasts	N1024L70 (12km horizontal resolution with 70 vertical levels)	00UTC: Day0 to Day10 12UTC: Day0 to Day 10	Up to 120 h
NEPS-G	Global Ensemble Prediction	N1024L70 (12 km horizontal resolution; Control+ 11 member)	00UTC: Day0 to Day10 12UTC: Day0 to Day10	Up to 120 h
NCUM-R	Regional domain (5-40°N and 65-100°E)	4 km resolution Explicit convection	00UTC: Day0 to Day3 12UTC: Day0 to Day3	Up to 72 h
NEPS-R	Regional Domain (7-38°N and 67-98°E)	4 km resolution (Control+ 11 member) Explicit convection	00UTC: Day0 to Day3	Up to 72 h

(ii) The bi-variate TC Tracker (MOTC Tracker):

The Met Office bi-variate approach for tracking TCs is used in real-time to track the location and intensity of the system in the models. The bi-variate method identifies TCs by examination of the 850RV field but then fixes the TC center to the nearest local MSLP minimum (Heming,2017). This is the adopted method at the Met Office, UK. The key advantage of the method is that it gives a strong signal of the approximate center of the TC even for weak systems and does not depend on the '*tcvitals*' information for tracking.

Appendix-II

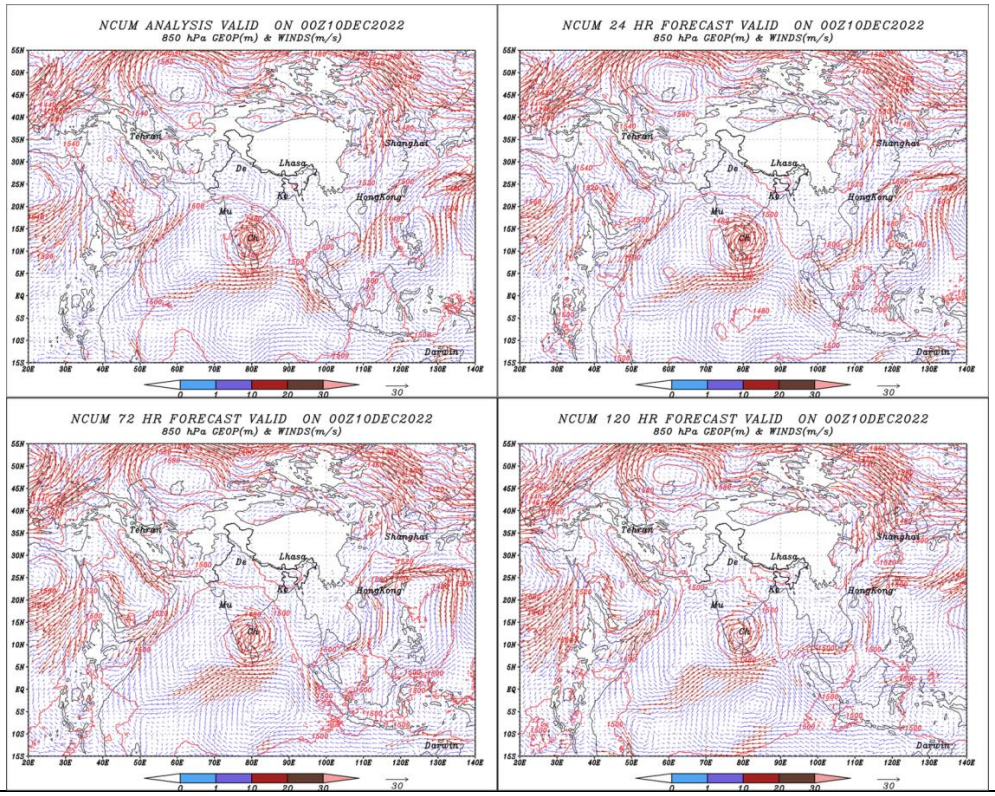

Figure A1. Analysis and forecast 850 hPa winds valid on 10th Dec 2022

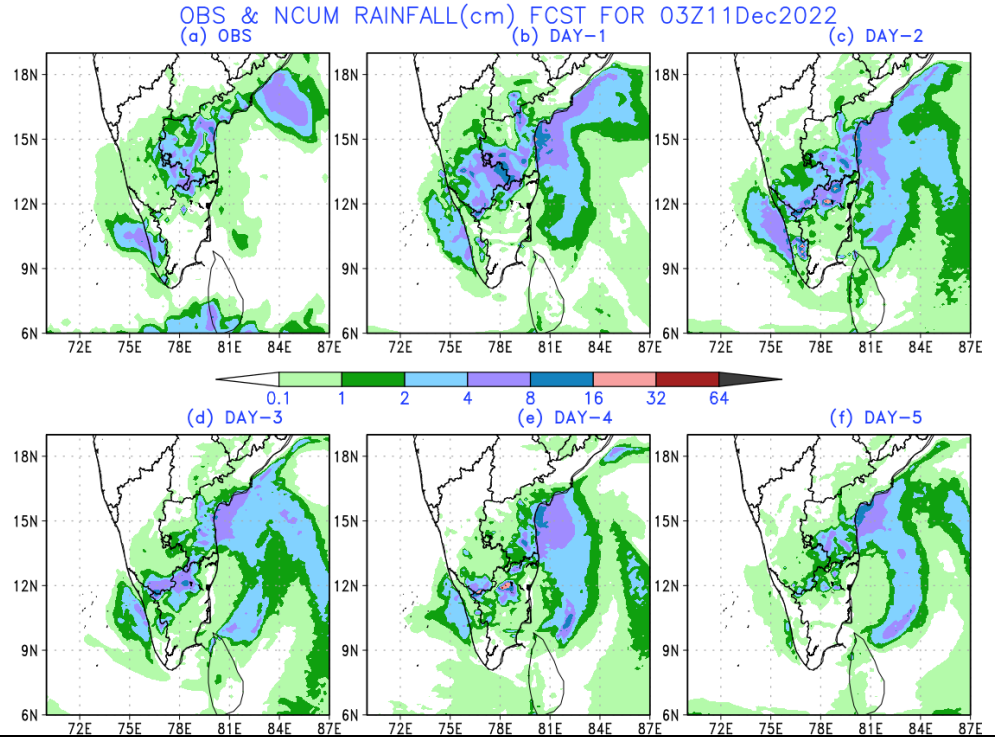

Figure A2. Observed and forecast 24h rainfall valid on 11th Dec 2022

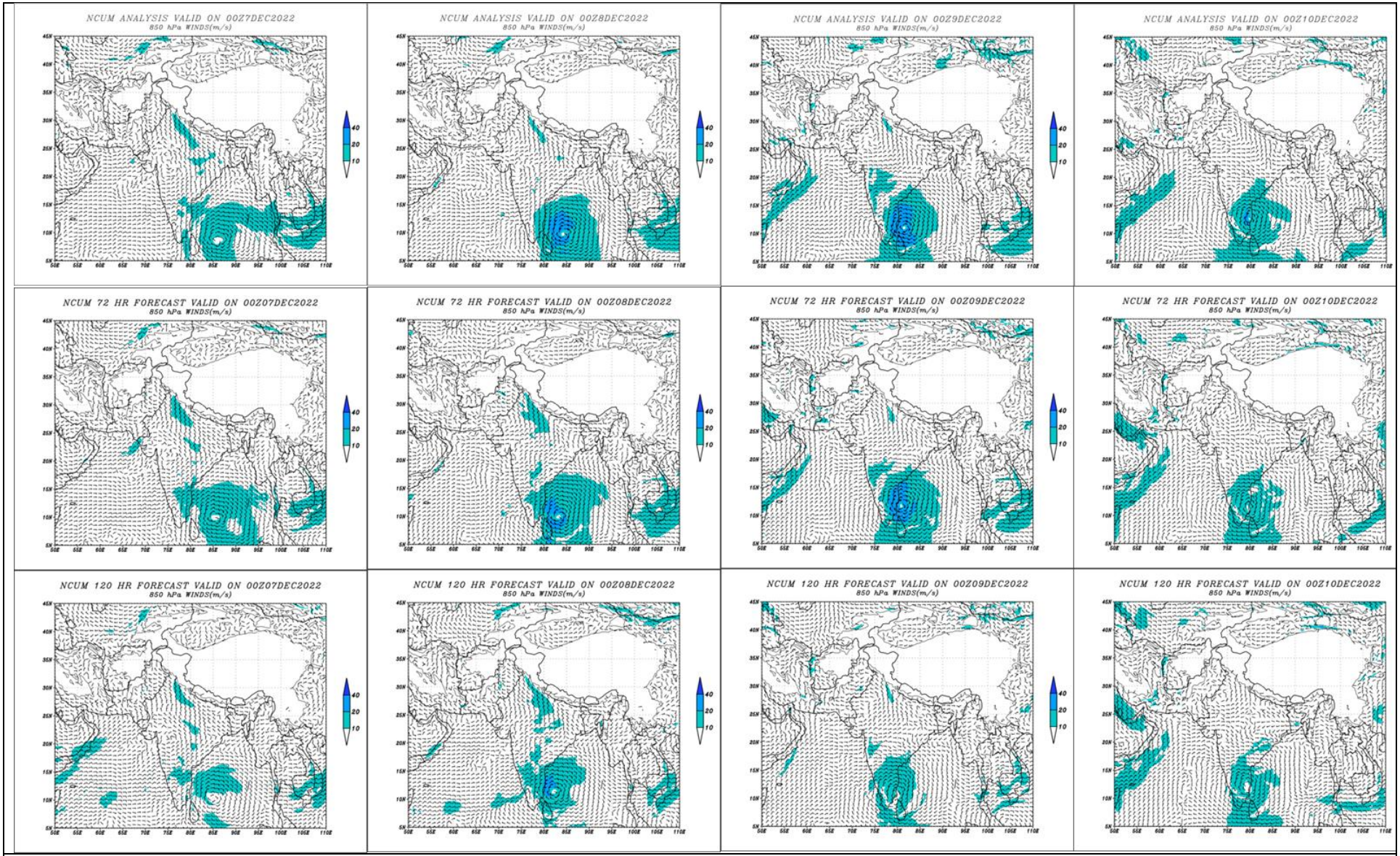

Figure A3 NCUM-G Analysis winds at 850 hPa during (7-10 Dec 2022; top row) compared with the corresponding Day-3 (middle row) and Day-5 forecasts (bottom)

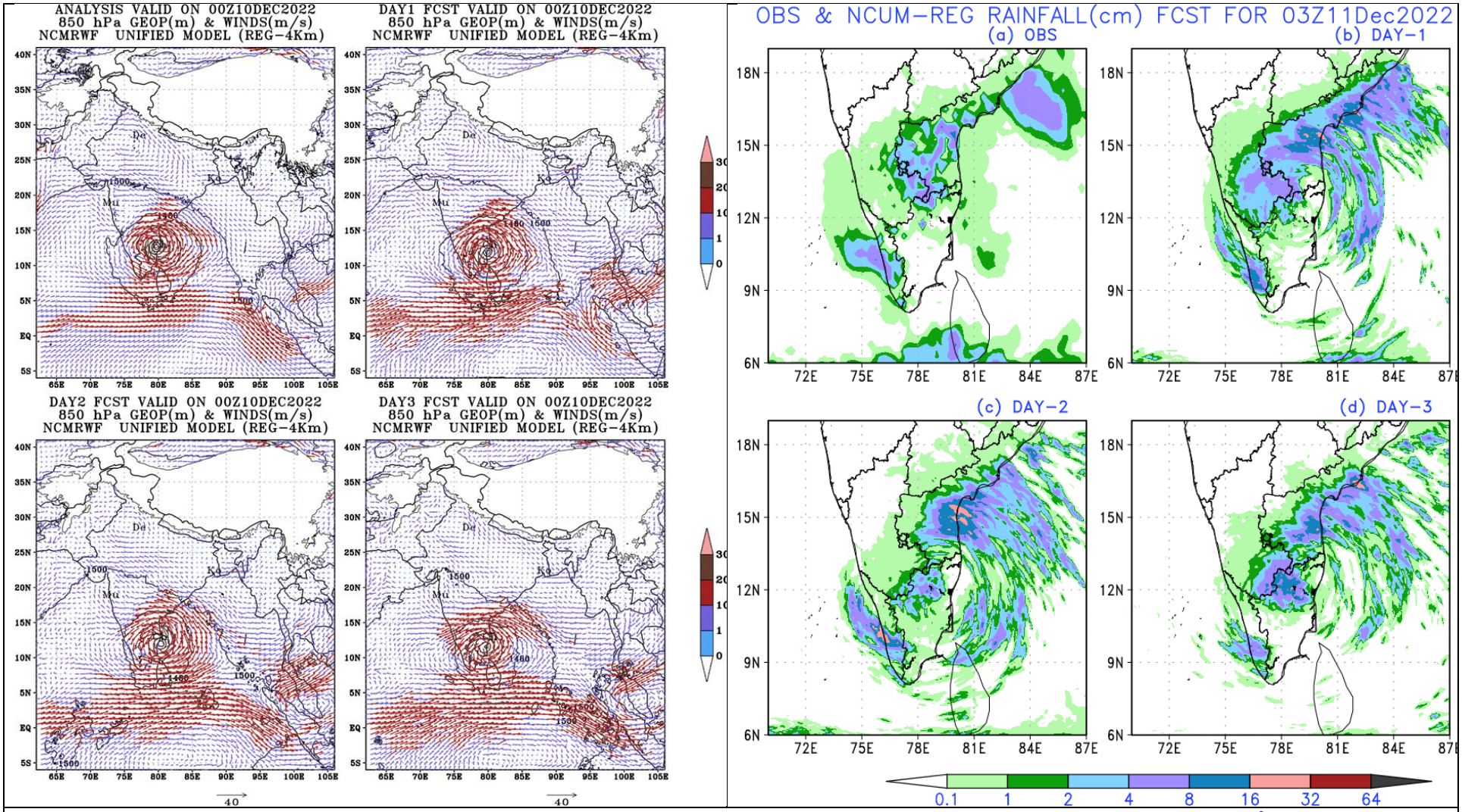

Figure A4 NCUM-R analysis and forecasts winds at 850 hPa (left) and observed and forecast rainfall valid on 10th Dec 2022